

Applications of the Generalized Wigner Distribution to Nanostructures on Surfaces: Universal Fluctuation Phenomena



Ted Einstein Physics, U. of Maryland, College Park
einstein@umd.edu <http://www2.physics.umd.edu/~einstein>

In collaboration with Alberto Pimpinelli, Rajesh Sathiyarayanan, Ajmi BHadj Hamouda, Kwangmoo Kim, Hailu Gebremariam, T.J. Stasevich, H.L. Richards, O. Pierre-Louis, S.D. Cohen, R.D. Schroll, N.C. Bartelt, and experimental groups of Ellen D. Williams & J.E. Reutt-Robey at UM, M. Giesen & H. Ibach at FZ-Jülich, & J.-J. Métois at Marseilles

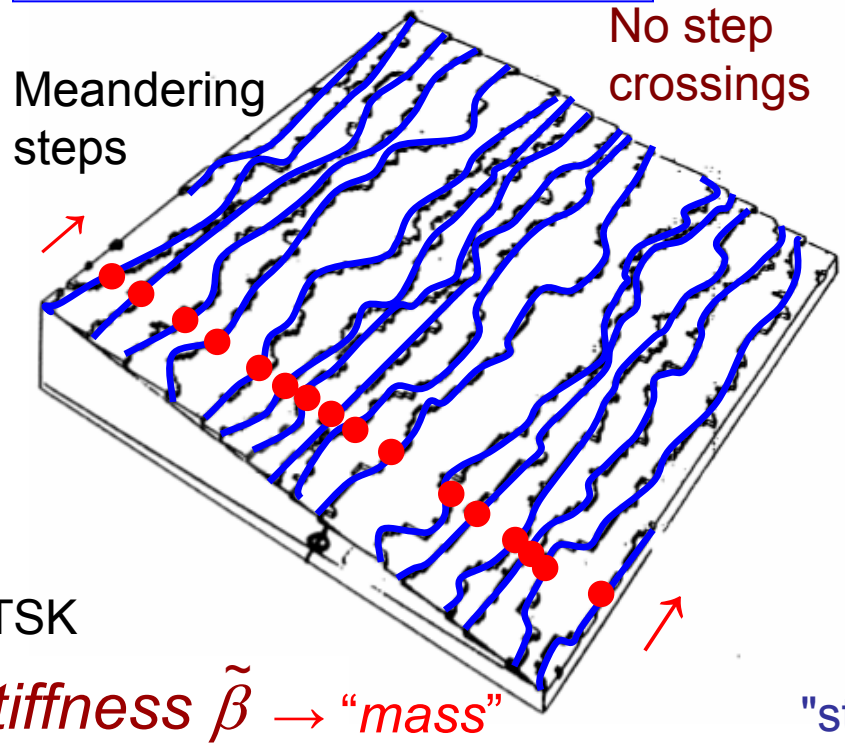
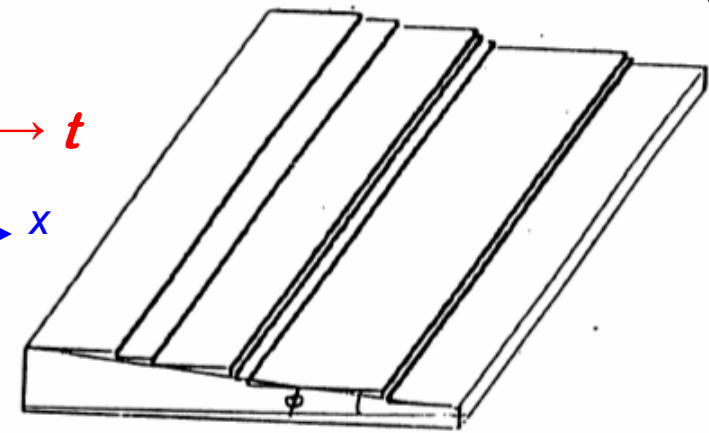
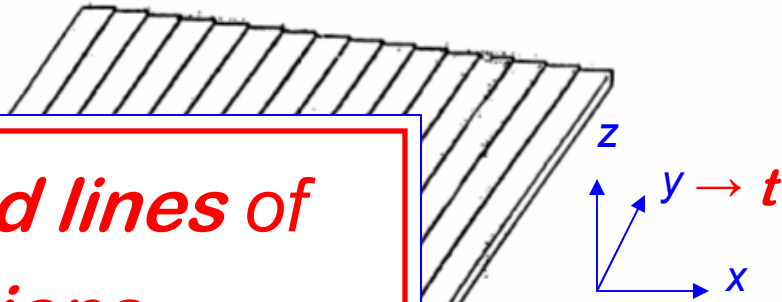
- Steps on vicinal surfaces as meandering fermions in (1+1)D...¿interactions?
- Reminder re terrace width distributions (TWDs), and what they reveal
- Relevance of random matrix theory— **universal features of fluctuations**
- **Generalizing the Wigner surmise** $P(s) = a s^{\varrho} e^{-bs^2}$ from symmetry-based: meaning of ϱ
- Possible corrections due to short-range effects
- Fokker-Planck formulation: study of relaxation to equilibrium
- **Scaling of capture zones of islands, quantum dots, etc.**

Terrace-Width Distribution $P(s)$ for Special Cases

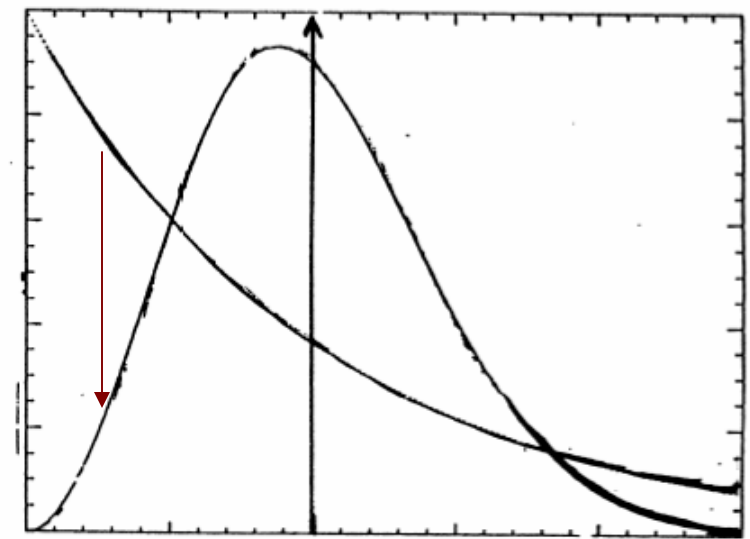
"Perfect Staircase" $\ell = \langle \ell \rangle \equiv 1/\tan \phi$ $s \equiv \ell / \langle \ell \rangle$

Straight steps, randomly placed
Geometric distribution: $P(s) = e^{-s}$

World lines of fermions evolving in 1D

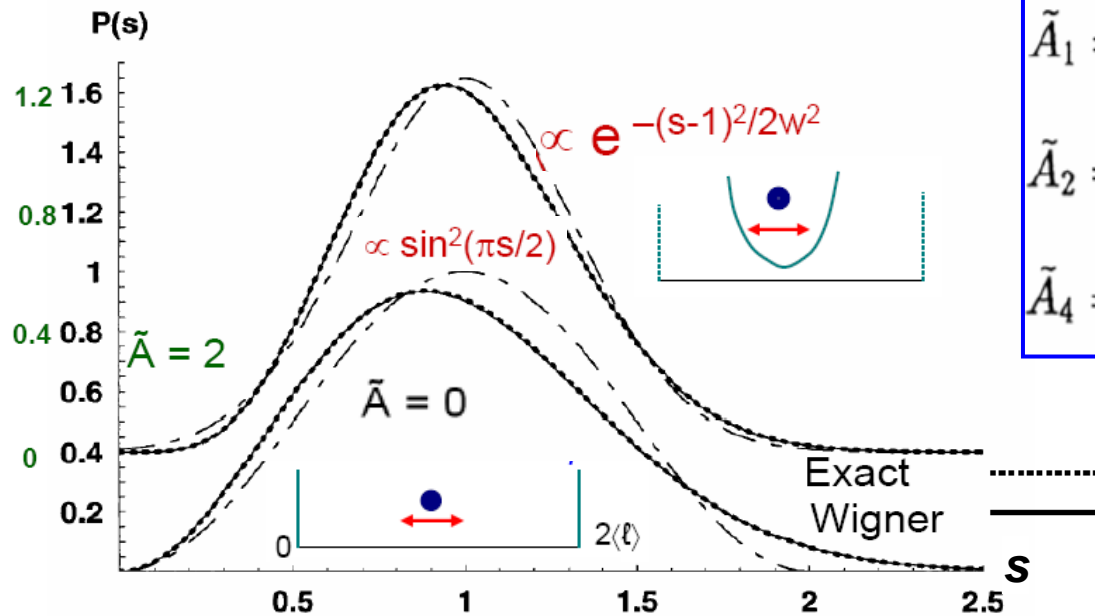


Scaled TWD: $P(s)$ indep. of $\langle \ell \rangle$



"static correlation" $\langle x_n(y) - x_{n-1}(y) - \langle \ell \rangle \rangle_{y,n}$

Wigner Surmise (WS) for TWD (terrace-width distribution)



$$\begin{aligned} \tilde{A}_1 = -1/4 : & \quad P_1(s) = \frac{\pi}{2} s \exp\left(-\frac{\pi}{4} s^2\right) \\ \tilde{A}_2 = 0 : & \quad P_2(s) = \frac{32}{\pi^2} s^2 \exp\left(-\frac{4}{\pi} s^2\right) \\ \tilde{A}_4 = 2 : & \quad P_4(s) = \left(\frac{64}{9\pi}\right)^3 s^4 \exp\left(-\frac{64}{9\pi} s^2\right) \end{aligned}$$

Generalizing from the special cases:

WS → GWS

- The three special cases correspond to $\varrho = 1, 2,$ and 4 .

- \tilde{A} and ϱ are related by: $\tilde{A} = (\varrho - 2)\varrho/4$;

$$\varrho = 1 + \sqrt{1 + 4\tilde{A}}$$

- Simplest interpolation expression:

$$P_\varrho(s) = a_\varrho s^\varrho \exp(-b_\varrho s^2)$$

- Two conditions on $P_\varrho(s)$: normalization & unit mean
 \Rightarrow values of a_ϱ, b_ϱ (in terms of Γ functions),

$$U(\ell) = A/\ell^2$$

$$\tilde{A} \equiv \frac{\tilde{\beta} A}{(k_B T)^2}$$

Physical Ideas Behind Application of Random Matrices

cf. T. Guhr, A. Müller-Groeling, H. A. Weidenmüller, Phys. Reports 299 ('98) 189 [cond-mat/97073]

Standard stat mech: ensemble of *identical* physical systems with *same* Hamiltonian but different initial conditions; Wigner: ensemble of dynamical systems governed by *different H's* with some common symmetry property, seeking generic properties of ensemble due to symmetry.

3 generic ensembles (Dyson) [with Gaussian weighting or circular]:

$\rho = 1$ *orthogonal* $H_{mn} = H_{nm} = H_{mn}^*$ time-reversal invariant with rotational symmetry

$\rho = 2$ *unitary* $H_{mn} = H_{mn}^\dagger$ time reversal violated (e.g. electron in B)

$\rho = 4$ *symplectic* $H = H^{(0)}_{mn} \begin{pmatrix} 1 & 0 \\ 0 & 1 \end{pmatrix} - i \sum_{j=1}^3 H^{(j)}_{mn} \sigma_j$; σ_j : Pauli spin matrices; $H^{(0)}$ real sym, $H^{(j)}$ real asym time-reversal invariant with 1/2-integer spin & broken rotational sym

GRMT useless for *average* quantities, but *fluctuations* for large number of levels becomes independent of the form of the level spectrum and of the Gaussian weight factors, and attains universal validity; can also derive from maximum entropy

OTHER APPLICATIONS of RMT

- Localization theory--ensemble of impurity potentials
- Transport in quasi-1D wires
- Fluctuations of persistent currents (esp. for non-interacting electrons)
- Level spectra of small metallic particles & their response to EM field
- Atomic nuclei, atoms and molecules
- Classical chaos (e.g. Bunimovich stadium, Sinai billiard)
- QCD, supersymmetry, 2D quantum gravity
- Classical chaos

Wigner's surmise: approximate $N \times N$ random matrices, $N \rightarrow \infty$, by 2×2 matrices.

Wigner's argument re Surmise

GOE (orthogonal): real, symmetric H , $N \times N$ matrix,

$$p(H) \sim \exp\left(-\frac{N}{\lambda_0^2} \text{tr}(H^2)\right), \quad N \rightarrow \infty$$

Opposite limit: $N = 2$, with ³ random elements h_{11} , h_{12} , & h_{22}

$$H = \begin{pmatrix} h_{11} & h_{12} \\ h_{12} & h_{22} \end{pmatrix} \quad \textit{splitting}$$

Let $\bar{h} \equiv (h_{11} + h_{22})/2$, $u \equiv h_{11} - h_{22}$, & $s \equiv (u^2 + 4h_{12}^2)^{1/2}$.

- Eigenvalues of H are $E_{2,1} = \bar{h} \pm s/2$ [independent of u]
- $h_{12} = \pm(s^2 - u^2)^{1/2}$
- $dh_{11} dh_{22} = d\bar{h} du$, $d\bar{h} ds = dE_1 dE_2$.

$$\begin{aligned} p(E_1, E_2) &\sim \exp\left(-\frac{2(E_1^2 + E_2^2)}{\lambda_0^2}\right) \int_{-s}^s du \left| \frac{dh_{12}}{ds} \right| \\ &= \frac{\pi}{2} (E_2 - E_1) \exp\left(-\frac{2(E_1^2 + E_2^2)}{\lambda_0^2}\right) \\ &\equiv \frac{\pi s}{2} \exp\left(-\frac{4\bar{h}^2 + s^2}{\lambda_0^2}\right) \end{aligned}$$

$$\Rightarrow p(s) = \int_{-\infty}^{\infty} d\bar{h} p(E_1, E_2) \sim s \exp(-s^2/\lambda_0^2) \quad \text{Wigner surmise}$$

Exact for $N = 2$ and excellent approximation as $N \rightarrow \infty$. For large N , the problem of level crossing ($s \rightarrow 0$) still reduces to a 2×2 problem near the (usually avoided) degeneracy.

To get $s = 0$, u and h_{12} must vanish simultaneously.

$$p(s) = \int du \int dh_{12} p(u, h_{12}) \delta\left(s - (u^2 + 4h_{12}^2)^{1/2}\right) \sim s, \quad s \ll 1$$

GUE (Gaussian unitary ensemble): H is hermitean, so that h_{12} is complex, and *three* parameters must vanish simultaneously to get $s = 0$: [4 random elements]

$$s = \left[(h_{11} - h_{22})^2 + 4(\Re h_{12})^2 + 4(\Im h_{12})^2\right]^{1/2}$$

Hence, $p(s) \sim s^2$, corresponding to a spherical (rather than circular) shell of radius s in parameter space.

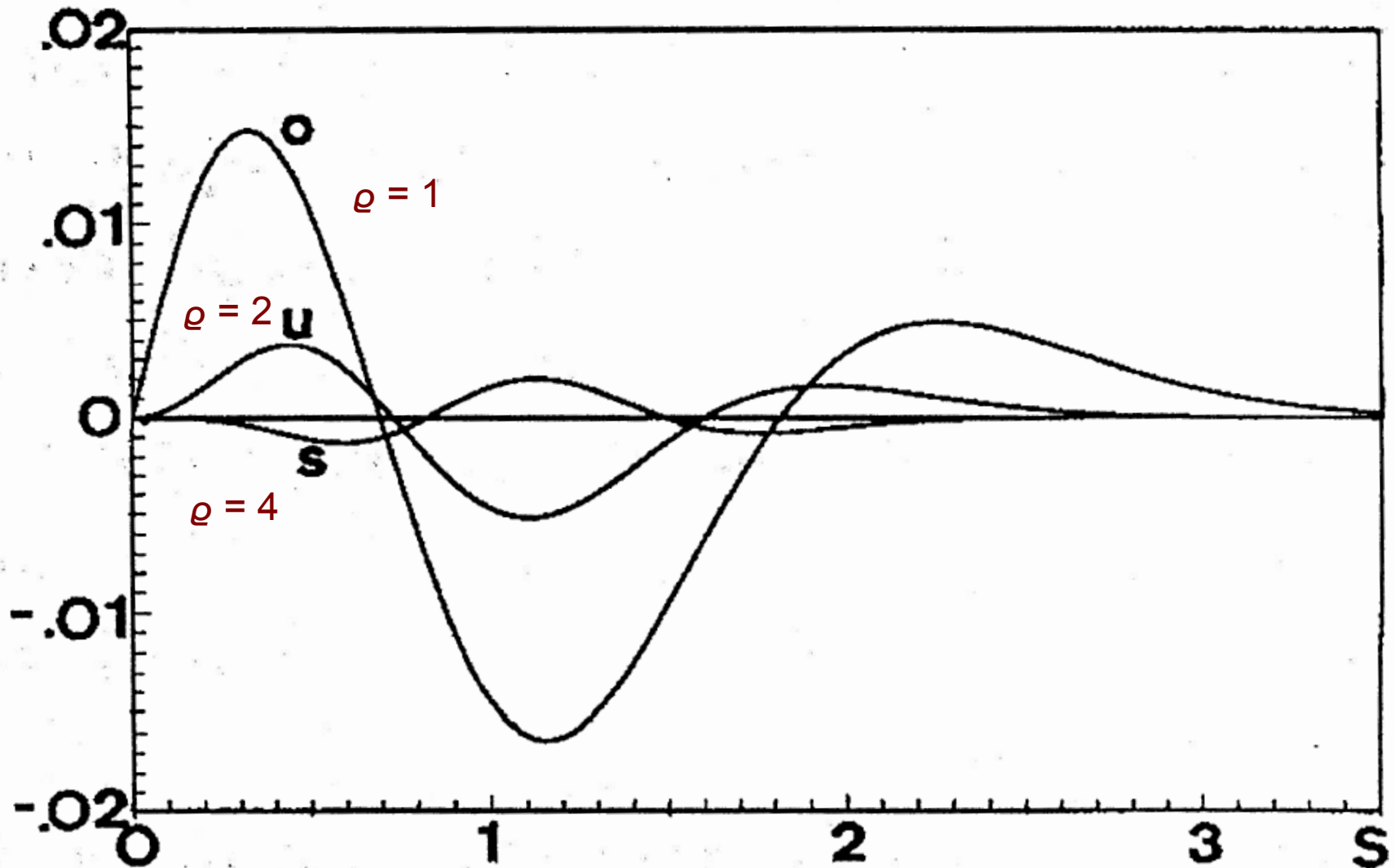
From W. Zwerger, "Theory of Coherent Transport," in T. Dittrich, ..., W. Zwerger, Quantum Transport and Dissipation (Wiley-VCH, Weinheim, 1998), chap. 1

Difference between exact solution & Wigner surmise for NN-spacing distribution

Wigner surmise [distribution] is an excellent approximation but not exact!

$P(s) - P^{\text{Wigner}}(s)$

from F. Haake, *Quantum Signatures of Chaos* ('92,'01)



Examples of NN spacing distributions with GOE ($\rho = 1$)

Fig. 1. Nearest-neighbor spacing distribution for the “Nuclear Data Ensemble” comprising 1726 spacings (histogram) versus $s = S/D$ with D the mean level spacing and S the actual spacing. For comparison, the RMT prediction labelled GOE and the result for a Poisson distribution are also shown as solid lines. Taken from Ref. [1].

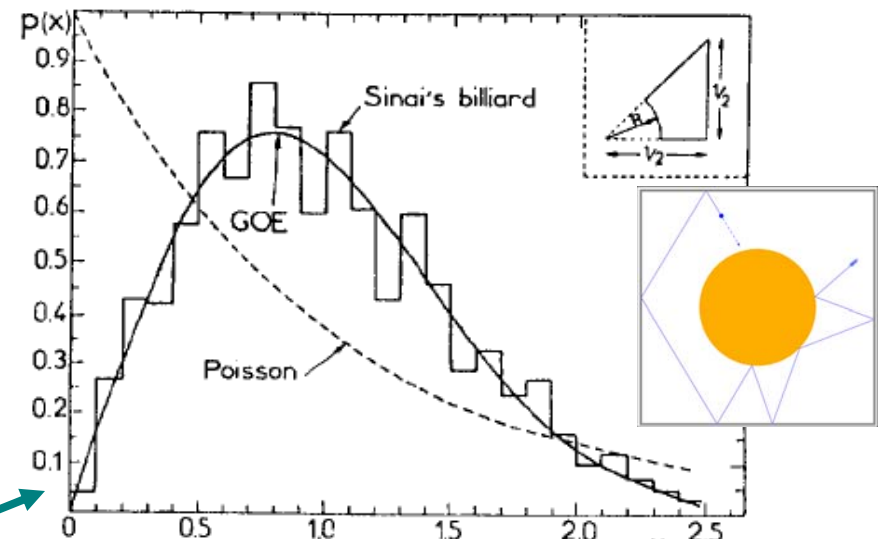
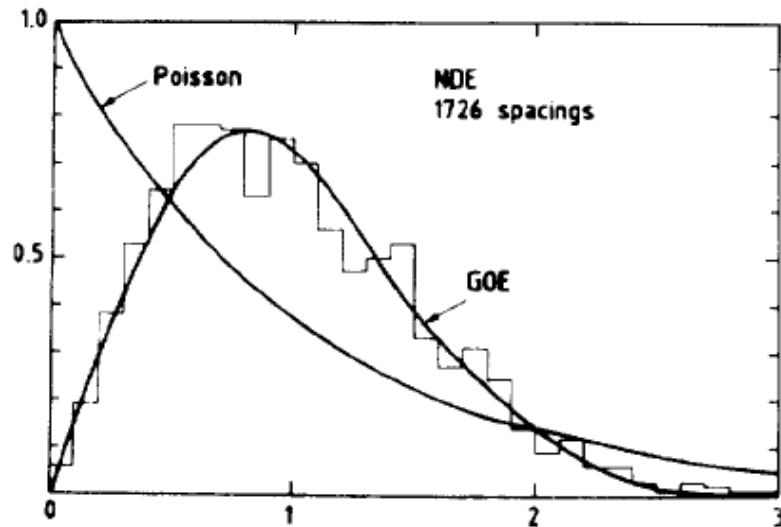


Fig. 4. The nearest-neighbor spacing distribution versus s (defined as in Fig. 1) for the Sinai's billiard. The histogram comprises about 1000 consecutive eigenvalues. Taken from Ref. [5].

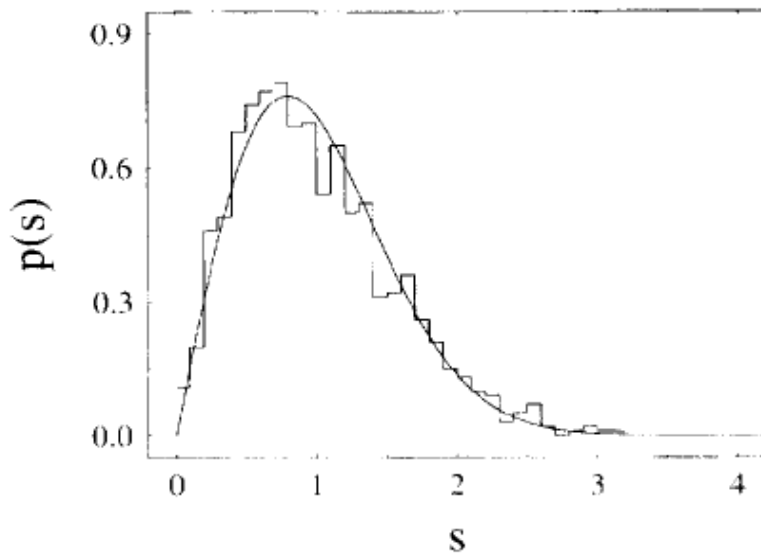


Fig. 6. Nearest-neighbor spacing distribution for elastomechanical modes in an irregularly shaped quartz crystal.

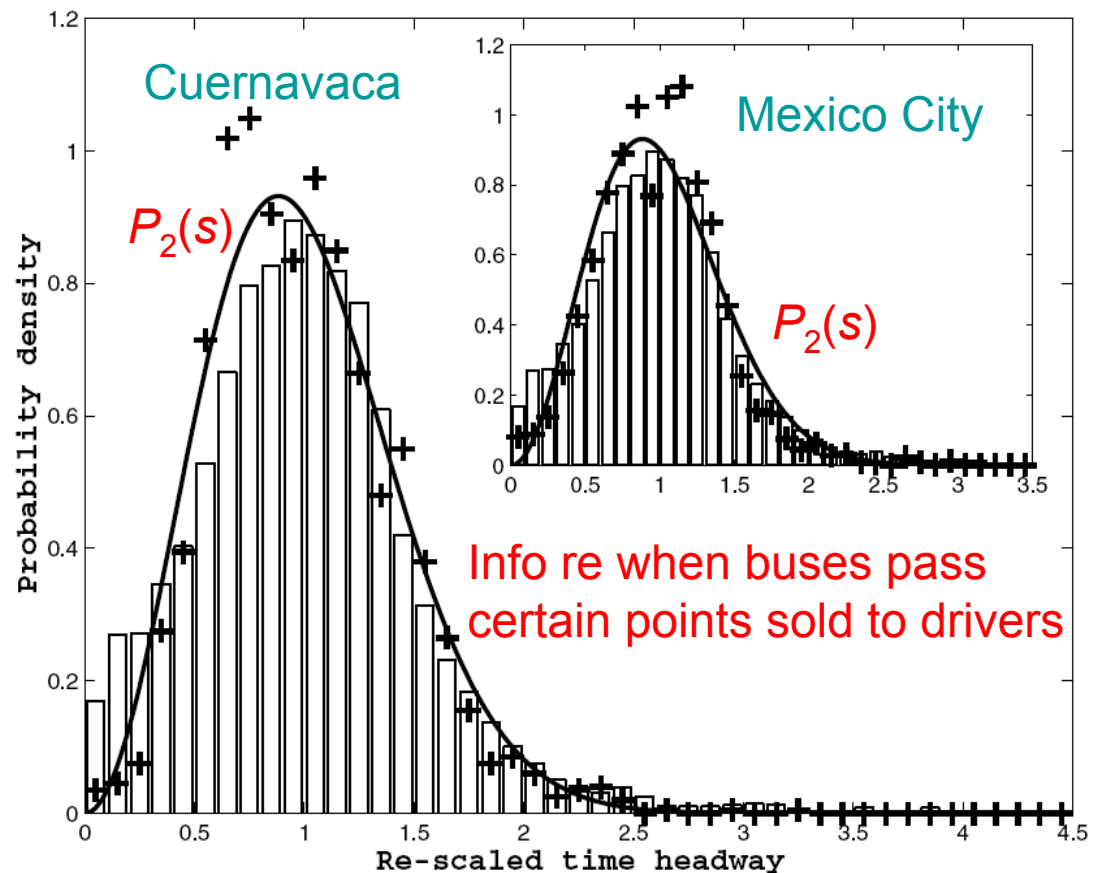
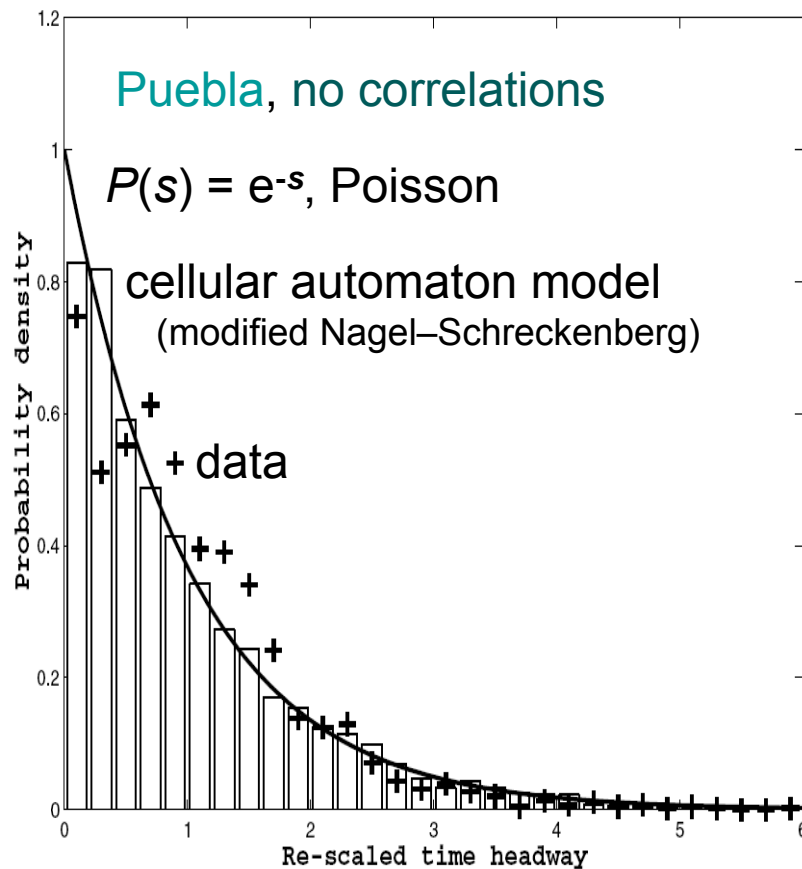
T. Guhr et al. / Physics Reports 299 (1998) 189

Headway statistics of buses in Mexican cities, using $P_2(s)$

M. Krbálek & P. Šeba, J. Phys. A **36** ('03) L7; **33** ('00) L229

Headway: time interval Δt between bus and next bus passing the same point

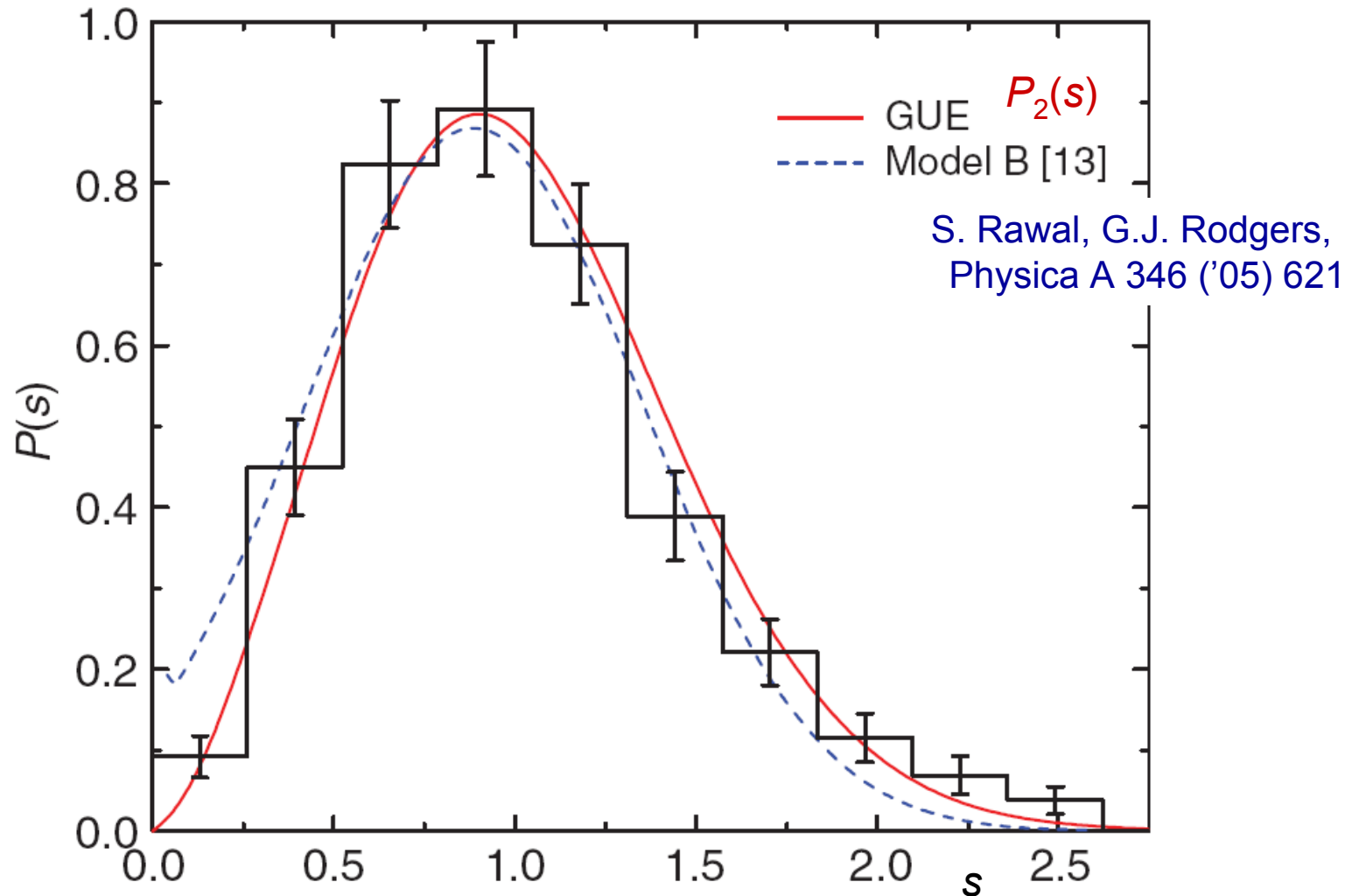
No timetable for buses in Mexico; independent drivers seek to optimize # riders/fares



WS $P_2(s)$ better than CA because in CA, correlations only between NNs

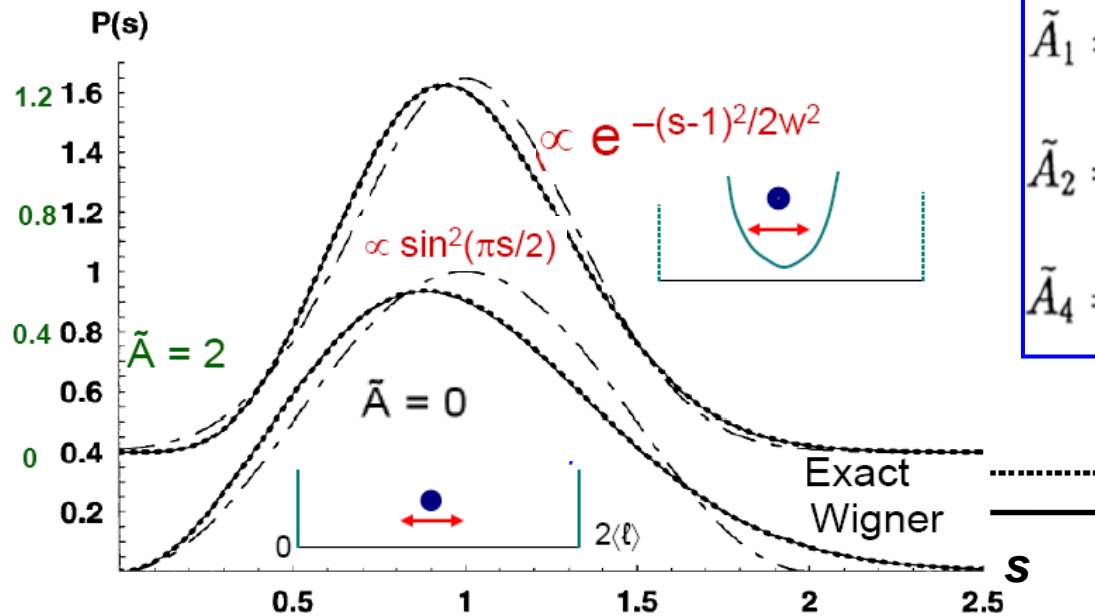
Modelling gap-size distribution of parked cars using RMT

A.Y. Abul-Magd, Physica A 368 ('06) 536



Unlike random sequential process, Coulomb gas extends repulsion beyond geometric size.

Wigner Surmise (WS) for TWD (terrace-width distribution)



$$\begin{aligned} \tilde{A}_1 = -1/4 : & \quad P_1(s) = \frac{\pi}{2} s \exp\left(-\frac{\pi}{4} s^2\right) \\ \tilde{A}_2 = 0 : & \quad P_2(s) = \frac{32}{\pi^2} s^2 \exp\left(-\frac{4}{\pi} s^2\right) \\ \tilde{A}_4 = 2 : & \quad P_4(s) = \left(\frac{64}{9\pi}\right)^3 s^4 \exp\left(-\frac{64}{9\pi} s^2\right) \end{aligned}$$

$$U(\ell) = A/\ell^2$$

$$\tilde{A} \equiv \frac{\tilde{\beta} A}{(k_B T)^2}$$

Generalizing from the special cases:

WS → GWS

- The three special cases correspond to $\varrho = 1, 2,$ and 4 .

- \tilde{A} and ϱ are related by: $\tilde{A} = (\varrho - 2)\varrho/4$; $\varrho = 1 + \sqrt{1 + 4\tilde{A}}$

- Simplest interpolation expression: $P_\varrho(s) = a_\varrho s^\varrho \exp(-b_\varrho s^2)$

- Two conditions on $P_\varrho(s)$: normalization & unit mean
 \Rightarrow values of a_ϱ, b_ϱ (in terms of Γ functions),

Calogero-Sutherland Model's Ground State & Random Matrices

Calogero-like Hamiltonian:

$$\mathcal{H} = -\sum_{j=1}^N \frac{\partial^2}{\partial x_j^2} + 2\frac{\beta}{2} \left(\frac{\beta}{2} - 1\right) \sum_{1 \leq i < j \leq N} (x_j - x_i)^{-2} + \omega^2 \sum_{j=1}^N x_j^2$$

[In the limit $N \rightarrow \infty$, $\omega \rightarrow 0$; in Calogero \mathcal{H} , $x_j^2 \rightarrow (x_j - x_i)^2$.]

$$\Psi_0 = \prod_{1 \leq i < j \leq N} |x_j - x_i|^{\varrho/2} \exp\left(-\frac{1}{2}\omega \sum_{k=1}^N x_k^2\right)$$



The ground-state density Ψ_0^2 is recognized as a joint probability distribution function from the theory of random matrices for Dyson's Gaussian ensembles.

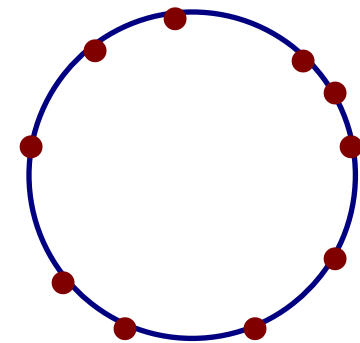
Sutherland Hamiltonian:

Miraculously, Ψ_0 of C-S models corresponds to that of RMT for cases $\varrho = 1, 2, \& 4$. But no need for $\varrho = 1 + (1+4\tilde{A})^{1/2}$ to have these values.

$$\mathcal{H} = -\sum_{j=1}^N \frac{\partial^2}{\partial x_j^2} + 2\frac{\beta}{2} \left(\frac{\beta}{2} - 1\right) \frac{\pi^2}{L^2} \sum_{i < j} \left[\sin \frac{\pi(x_j - x_i)}{L} \right]^{-2}$$

$$\Psi_0 = \prod_{i < j} \left| \sin \frac{\pi(x_j - x_i)}{L} \right|^{\varrho/2}, \quad x_j > x_i$$

$$\theta_i \equiv 2\pi x_i/L \Rightarrow \Psi_0^2 = \prod_{i < j} |e^{i\theta_j} - e^{i\theta_i}|^{\varrho}$$



The ground-state density Ψ_0^2 is also a joint probability distribution function from the theory of random matrices, now for Dyson's circular ensembles.

Note that the pair correlation functions and other properties of the ensembles can be evaluated exactly only for the cases $\beta = 1, 2$, or 4 , corresponding to orthogonal, unitary, or symplectic symmetry of the ensemble.

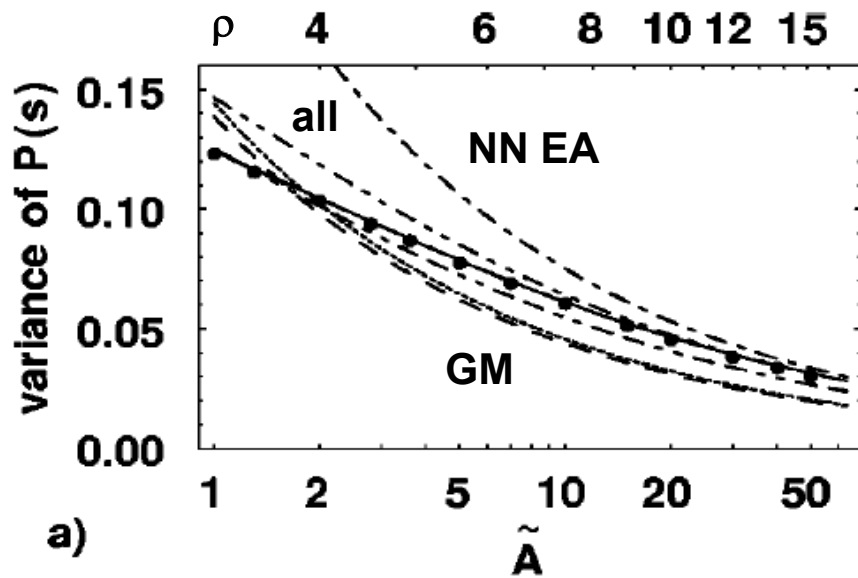
Comparison of variance of $P(s)$ vs. \bar{A} computed with Monte Carlo:
GWS does **better**, quantitatively & conceptually, than any other approximation

Hailu Gebremariam et al., Phys. Rev. B 69 ('04)125404

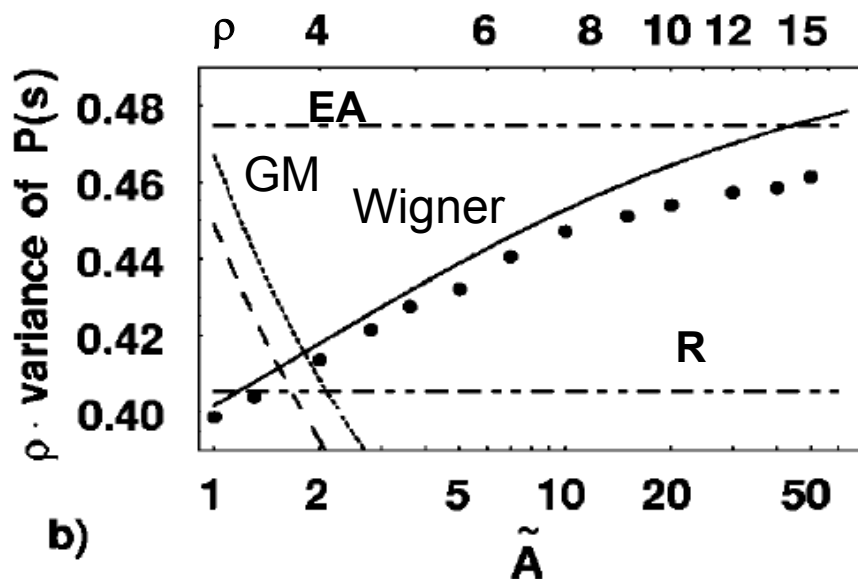
Experiments measuring variances of TWDs

Vicinal	T (K)	σ^2	ϱ	\bar{A}	A_W/A_G	A_W (eV Å)	Experimenters
Pt(1 1 0)-(1 × 2)	298		2.2	0.13	–	$\bar{\beta} = ?$	Swamy, Bertel [36]
Cu(1 9, 17, 17)	353	0.122	4.1	2.2	0.77	0.005	Geisen [5,54]
Si(1 1 1)	1173	0.11	3.8	1.7	0.96	0.4	Bermond, Métois [55]
Cu(1, 1, 13)	348	0.091	4.8	3.0	1.27	0.007	Giesen [5,56]
Cu(11,7,7)	306	0.085	5.1	4	1.37	0.004	Geisen [5,54]
Cu(1 1 1)	313	0.084	5.0	3.6	1.39	0.004	Geisen [5,54]
Cu(1 1 1)	301	0.073	6.0	6.0	1.58	0.006	Geisen [5,54]
Ag(1 0 0)	300	0.073	6.4	6.9	1.58	$\bar{\beta} = ?$	P. Wang...Williams
Cu(1, 1, 19)	320	0.070	6.7	7.9	1.64	0.012	Geisen [5,56]
Si(1 1 1)-(7 × 7)	1100	0.068	6.4	7.0	1.67	0.7	Williams [57]
Si(1 1 1)-(1 × 1)Br	853	0.068	6.4	7.0	1.67	0.1	X.-S. Wang, Williams [58]
Si(1 1 1)-Ga	823	0.068	6.6	7.6	1.67	1.8	Fujita...Ichikawa [59]
Si(1 1 1)-Al $\sqrt{3}$	1040	0.058	7.6	10.5	1.85	2.2	Schwennicke...Williams [60]
Cu(1, 1, 11)	300	0.053	8.7	15	1.95	0.02	Barbier et al. [21]
Cu(1, 1, 13)	285	0.044	10	20	2.12	0.02	Geisen [5,56]
Pt(1 1 1)	900	0.020	24	135	2.59	6	Hahn...Kern [61]
Si(1 1 3) rotated	1200	0.004	124	3.8×10^3	2.92	$(27 \pm 5) \times 10^2$	van Dijken, Zandvliet, Poel-sema [9]

Monte Carlo data confronts approximations



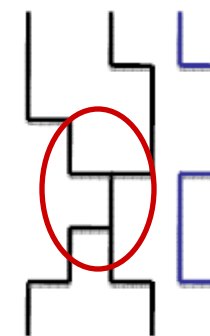
Dots: MC data
 Line: Wigner
 Dashes: Gruber-Mullins (mean field)
 Long-short [-short]: Grenoble
 (no entropic int'n, EA)
 Long-long-short-short: Saclay
 (continuum roughening, R)



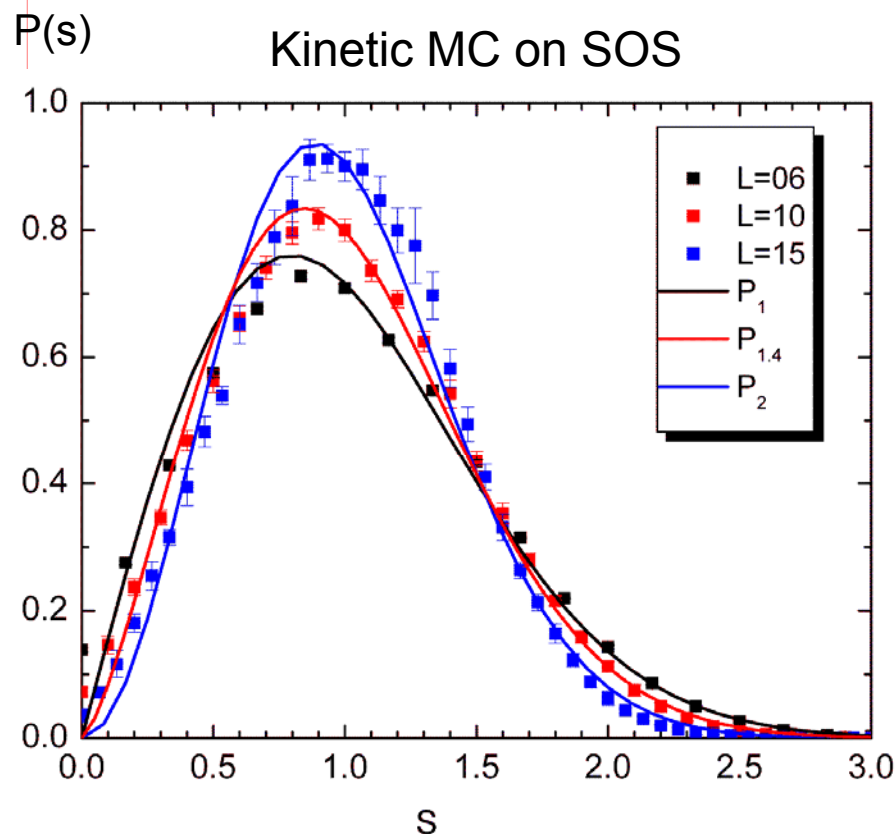
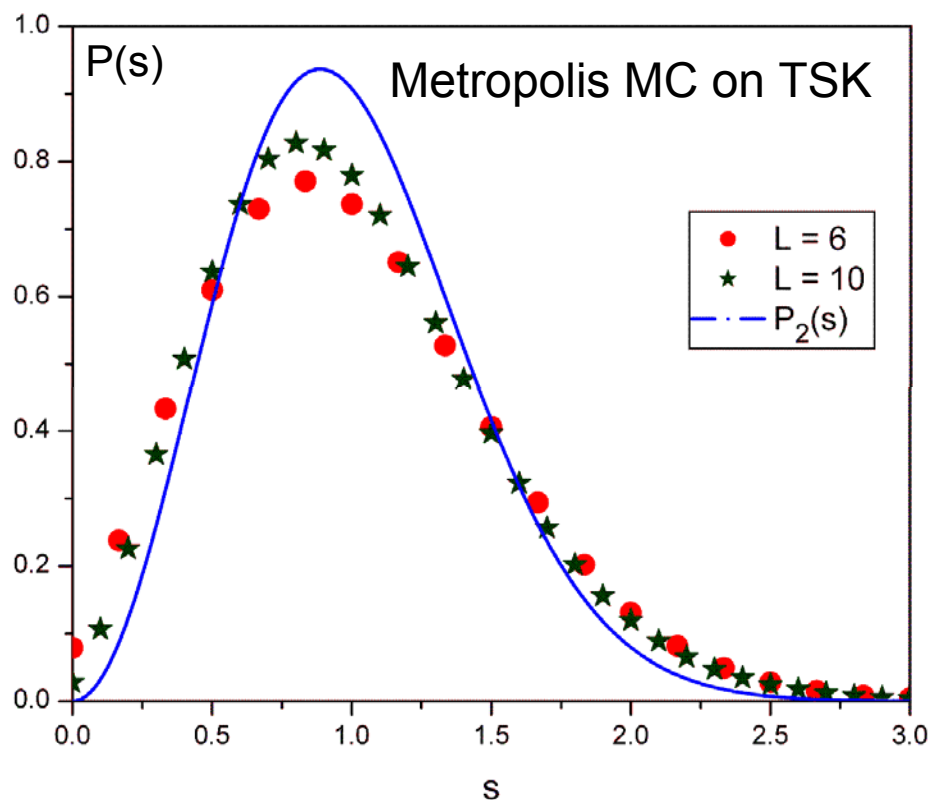
Lower plot highlights differences:
 remove ρ^{-1} asymptotic decay
 Wigner is best, quantitatively
 and conceptually

Hailu Gebremariam et al.,
 Phys. Rev. B 69 ('04)125404

What happens when steps are allowed to touch?
Effective attraction: $\varrho = 2 \rightarrow \varrho < 2$, finite-size dep.



Rajesh Sathiyarayanan, Ajmi BH Hamouda



L	6	8	10	12	16
$\varrho(L)$	1	1.3	1.3	1.4	1.45
\tilde{A}	-0.25	-0.23	-0.23	-0.21	-0.20

$T = 580 \text{ K}$

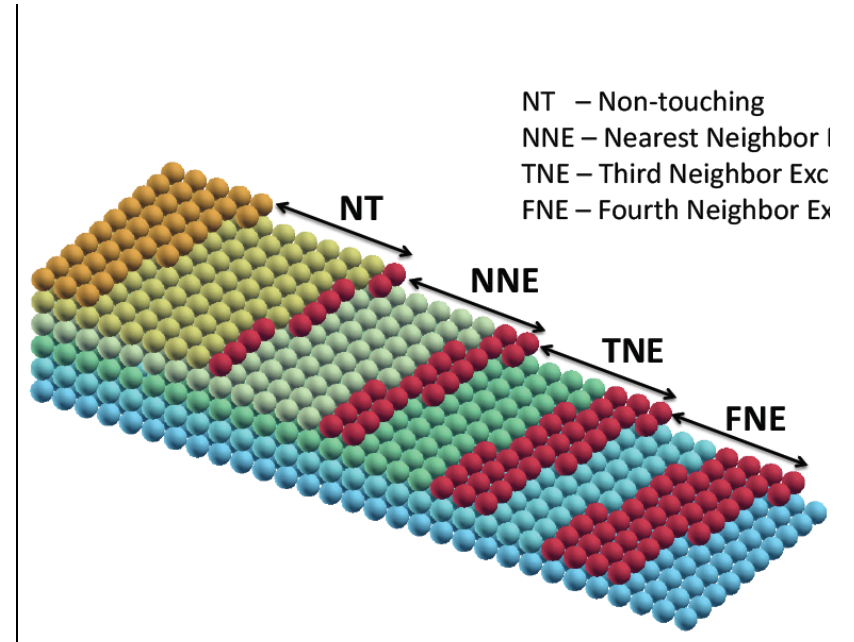
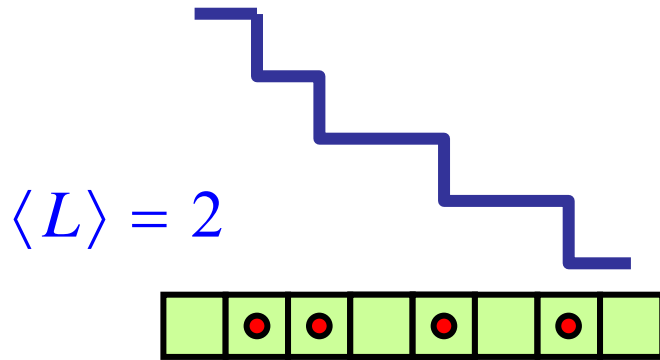
$E_d = 1 \text{ eV}$

$E_a = 0.35 \text{ eV}$

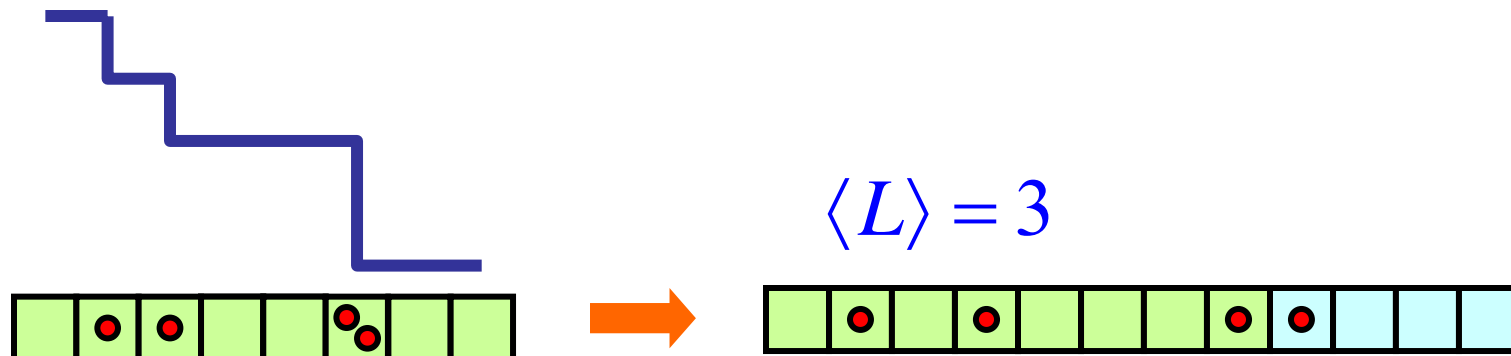
NNI (NT) and NN2 Chains

Kwangmoo Kim

- Map steps onto 1D free-fermions



- Overlapping steps (NN2) can be mapped onto Nearest-Neighbor Included (NNI) chain, then *shifted* and *rescaled*



NNE : S.-A. Cheong & C. L. Henley (unpublished); S.-A. Cheong, dissertation

Why Look for Fokker-Planck Equation for TWD?

- Justification/derivation of generalized continuum Wigner surmise since no symmetry basis for $\varrho \neq 1, 2, \text{ or } 4$
- Dynamics: how non-equilibrium TWD (e.g. step bunch) evolves toward equilibrium
- Quench or upquench: sudden change of T does not change A much but changes \tilde{A} (and so ϱ) considerably
- Connections with other problems, e.g. capture zone distribution (& Heston model of econophysics)

Derivation of Fokker-Planck for TWD

- Start with Dyson Coulomb gas/Brownian motion model: repulsions $\propto 1/(\text{separation})$ & parabolic well

$$\dot{x}_i = -\gamma x_i + \sum_{i \neq j} \frac{\hat{q}}{x_i - x_j} + \sqrt{\Gamma} \eta$$

- Assume steps beyond nearest neighbors are at integer times mean spacing (cf. Gruber-Mullins)

$$\dot{s} = -\kappa s + \rho/s + \text{noise}$$

Noise sets time scale.

$$\tilde{t} \equiv t \Gamma / \langle \ell \rangle^2 \quad \boxed{1/\tau}$$

- Demand self-consistency for width of parabolic confining well: $\kappa \rightarrow 2b_\rho$

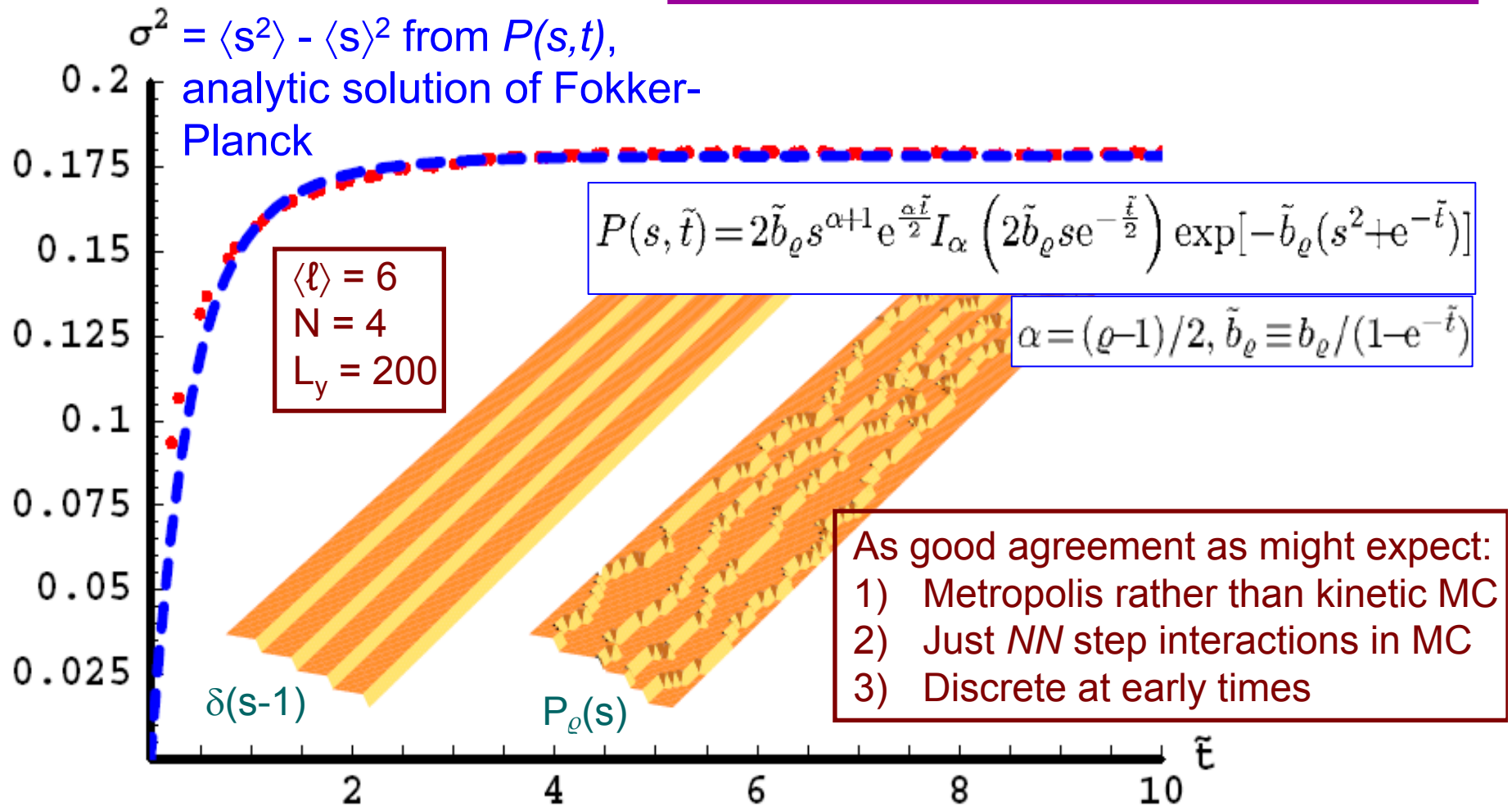
$$\frac{\partial P(s, \tilde{t})}{\partial \tilde{t}} = \frac{\partial}{\partial s} \left[\left(2b_\rho s - \frac{\rho}{s} \right) P(s, \tilde{t}) \right] + \frac{\partial^2}{\partial s^2} [P(s, \tilde{t})] \rightarrow P_\rho(s)$$

Check of Fokker-Planck with Monte Carlo

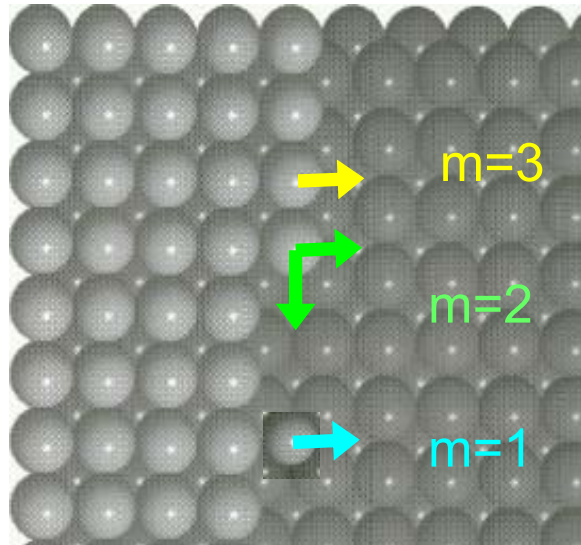
cleaved \rightarrow equilibrium

TSK model (no adatom carriers)

Best match for 1.4 FP time units = 10^3 MCS



Improved tests: Kinetic MC & SOS model

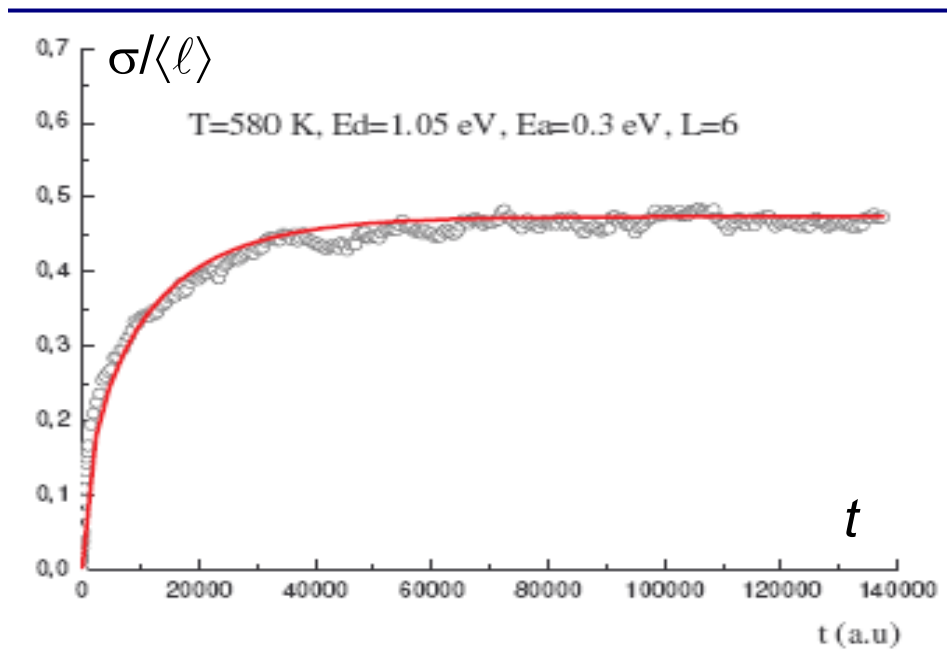


$$E_{\text{barrier}} = E_d + m E_a \quad \text{breaking } m \text{ bonds}$$

$$E_d = 0.9 - 1.1 \text{ eV}; E_a = 0.3 - 0.4 \text{ eV}$$

$$T = 520 - 580 \text{ K}$$

$$\langle \ell \rangle = 4-15, 5 \text{ steps}, 10000 \times L_x$$



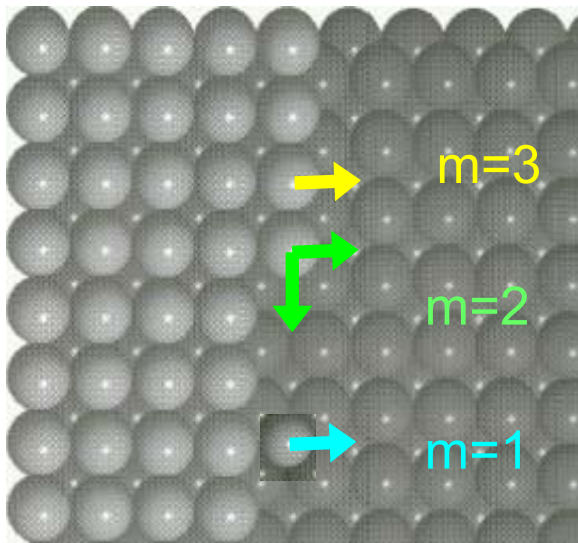
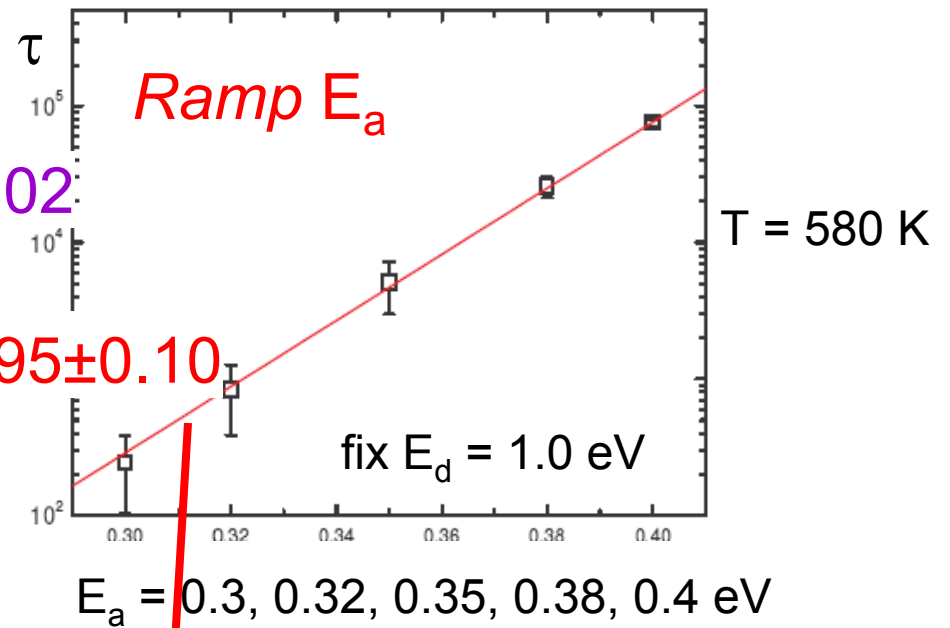
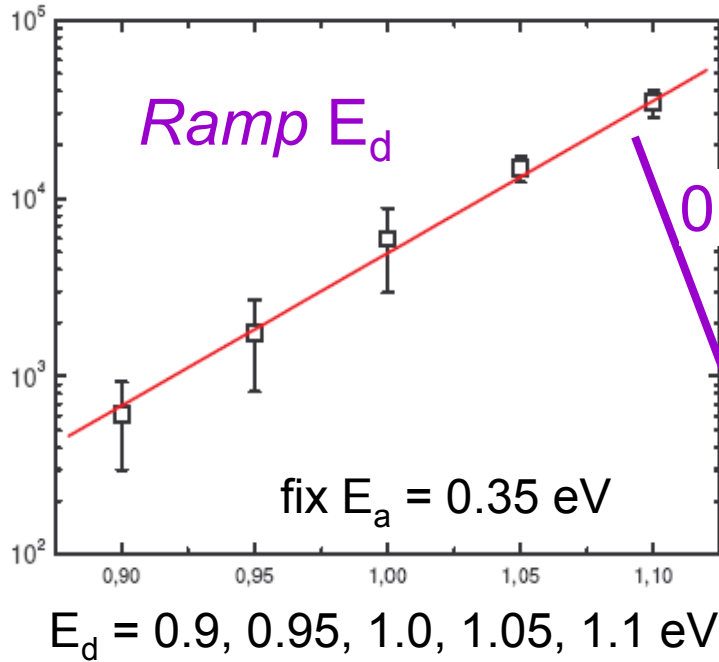
Fit:

$$\sigma(t) = \sigma_{\text{sat}} \sqrt{1 - \exp(-t / \tau)}$$

Expect $\tau \propto \exp(E_{\text{barrier}} / k_B T)$

$$\text{Find } E_{\text{barrier}} \approx 1 E_d + 3 E_a$$

Behavior of τ in SOS via KMC: Ramp E_d , E_a , T , $\langle \ell \rangle$



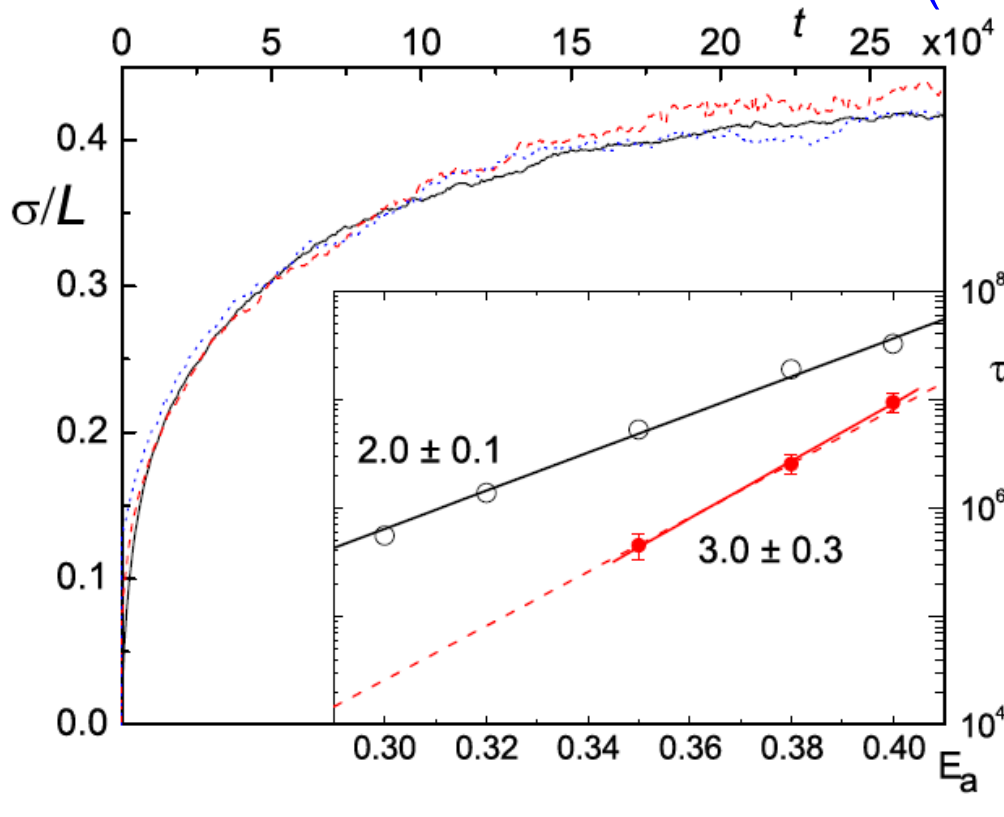
$$E_{\text{barrier}} = 1 E_d + 3 E_a$$

Kink-antikink creation (edge detachment) is rate-limiting!

Ramp T (520 \rightarrow 580K) with $E_a=0.3$ eV, $E_d=1.0$ eV
 \Rightarrow activation energy = $(0.989 \pm 0.005)(E_d+3E_a)$

$\tau = \langle \ell \rangle^2 / \Gamma$, ramp $\langle \ell \rangle^2$: slope OK (18% below expected)

Further checks to confirm that $m=3$ (kink-antikink creation) determines rate

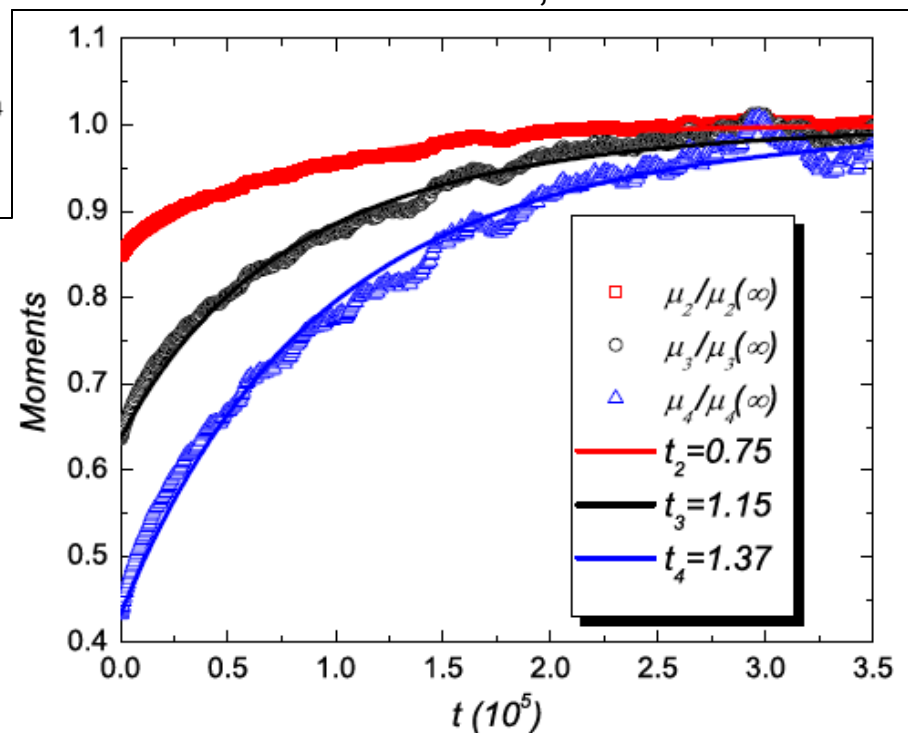


Main graph:

Evolution of 3 different initial conditions: straight, “decimated”, and crenelated. Comparable results, even though initial burst atoms from crenelated.

Inset: Surface azimuthally misoriented, 5 forced kinks in 10^4 sites. Kinks initially 2000 sites apart, as before. With $m=3$ moves frozen, slower.

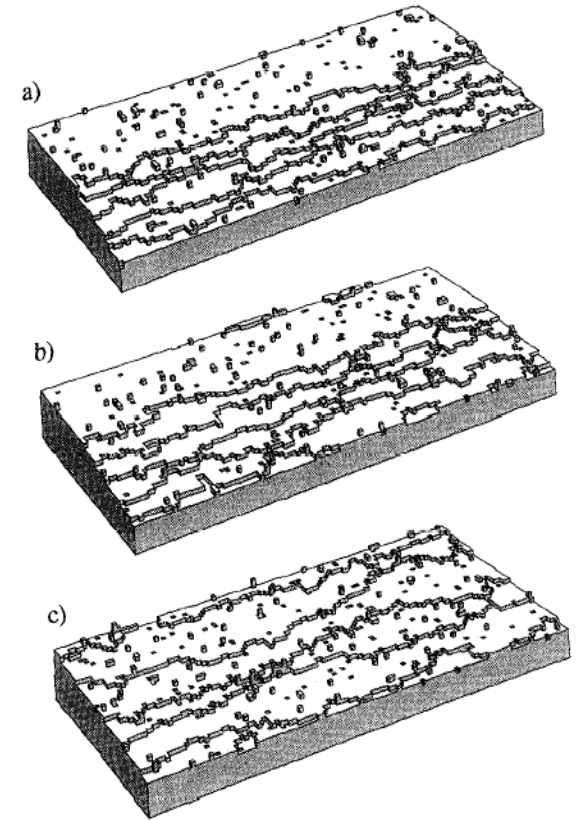
Higher moments, not just variance, consistent with analytic predictions from F-P (characterized in detail)!



2 other situations of interest

Step Bunch: initially a delta function

$$P(s, \tilde{t}) \rightarrow \frac{a_\varrho s^\varrho}{(1 - e^{-\tilde{t}})^{(\varrho+1)/2}} \exp[-s^2 b_\varrho / (1 - e^{-\tilde{t}})]$$



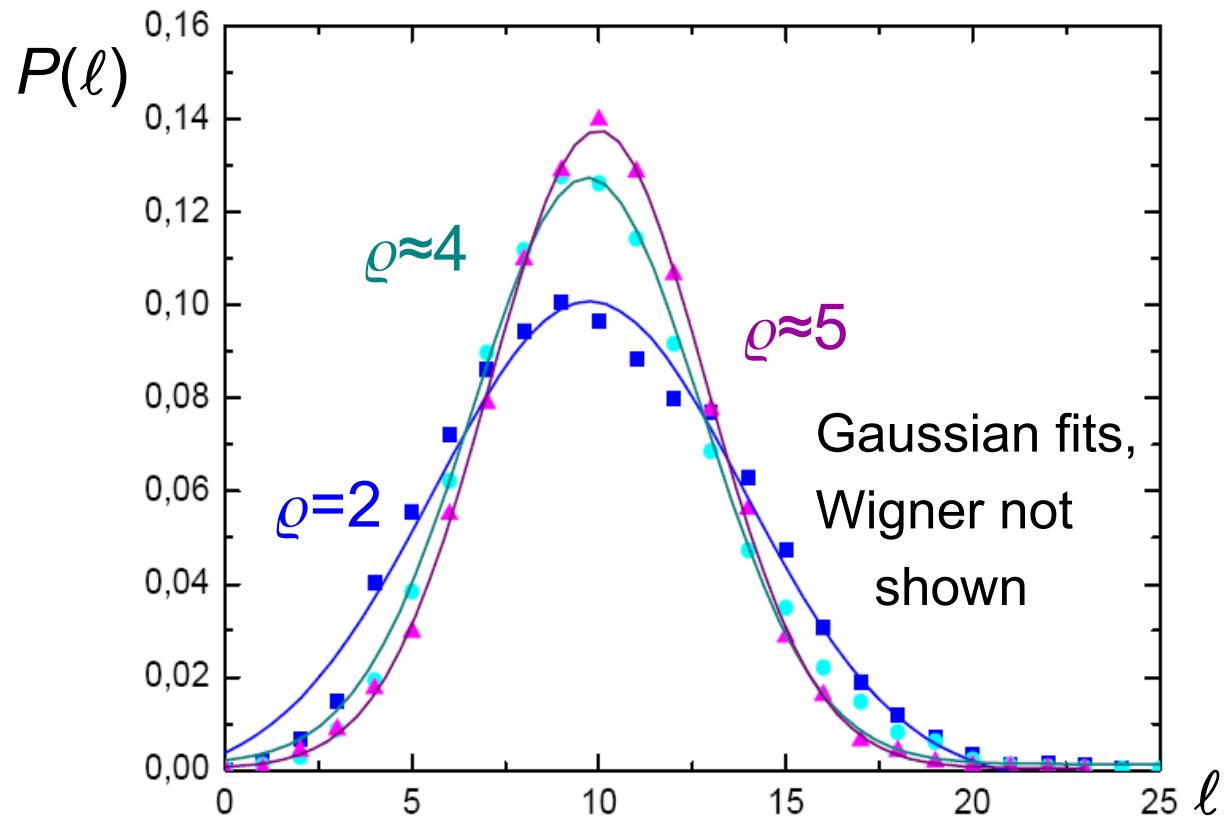
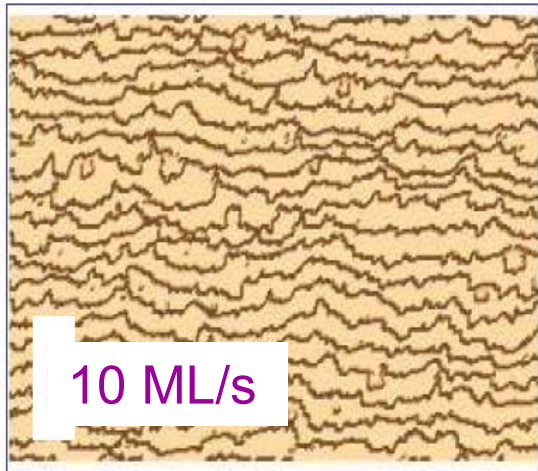
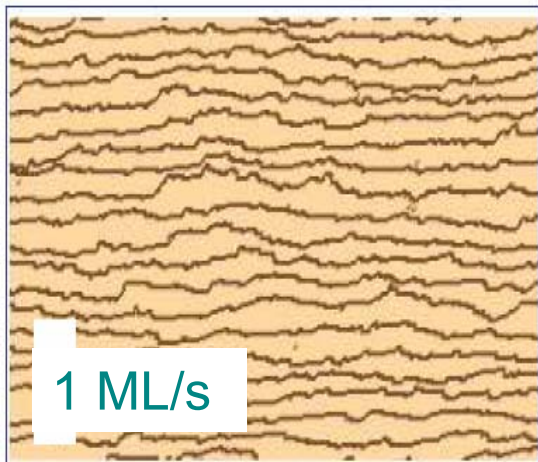
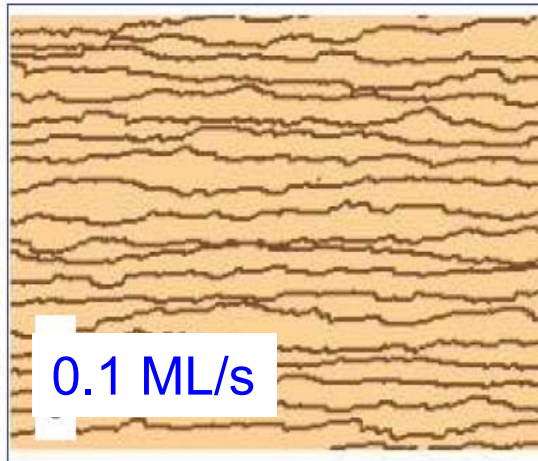
Quench or upquench: change from initial ρ_0 to ρ , e.g. change in temperature

$$P(s, \tilde{t}) = a_\varrho s^\varrho e^{-\tilde{b}_\varrho s^2} \frac{(1 - e^{-\tilde{t}})^{\frac{\varrho_0 - \varrho}{2}}}{(1 - e^{-\tilde{t}}(1 - b_\varrho/b_{\varrho_0}))^{\frac{\varrho_0 + 1}{2}}} {}_1F_1 \left(\frac{\varrho_0 + 1}{2}, \frac{\varrho + 1}{2}, \frac{\tilde{b}_\varrho s^2}{1 + (b_{\varrho_0}/b_\varrho)(e^{\tilde{t}} - 1)} \right)$$

Final

Does growth flux (step motion) alter TWD?

Test: *no energetic interaction* ($\varrho=2$), 150 ML



- Narrower \Rightarrow *effective* repulsion that rises with flux, higher ϱ , more Gaussian-like
- Decreased apparent stiffness $\tilde{\beta}$

20 steps, 1000x200, $T=723\text{K}$, $E_d=1.0\text{eV}$, $E_a=0.3\text{eV}$

...or etching ? (non-equilibrium steady state)

from S. P. Garcia, H. Bao, & M. A. Hines, "Effects of Diffusional Processes on Crystal Etching: Kinematic Theory (KT) Extended to 2D," *J. Phys. Chem. B* **108** (2004) 6062

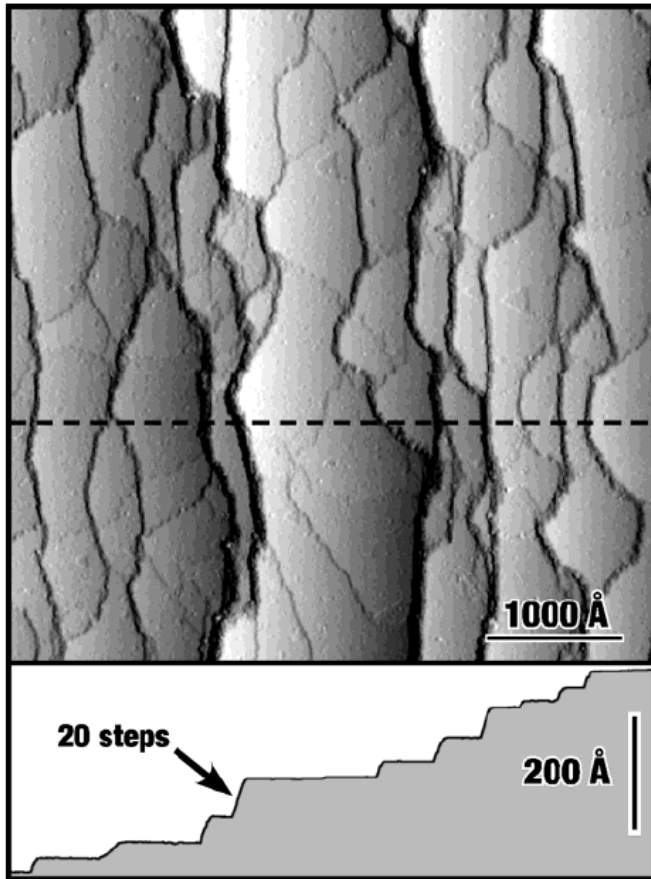


Figure 1. STM image of a Si(111) surface miscut by 3.5° in the $\langle 11\bar{2} \rangle$ direction after etching for 5 min in an unstirred, room temperature, 50% (w/v) aqueous KOH solution. Although pronounced macrostep formation is visible, there are also many "crossing steps" connecting the macrosteps. A cross-sectional slice is indicated by the dashed line and displayed in the lower panel. No consistent preference for concavity or convexity is observed.

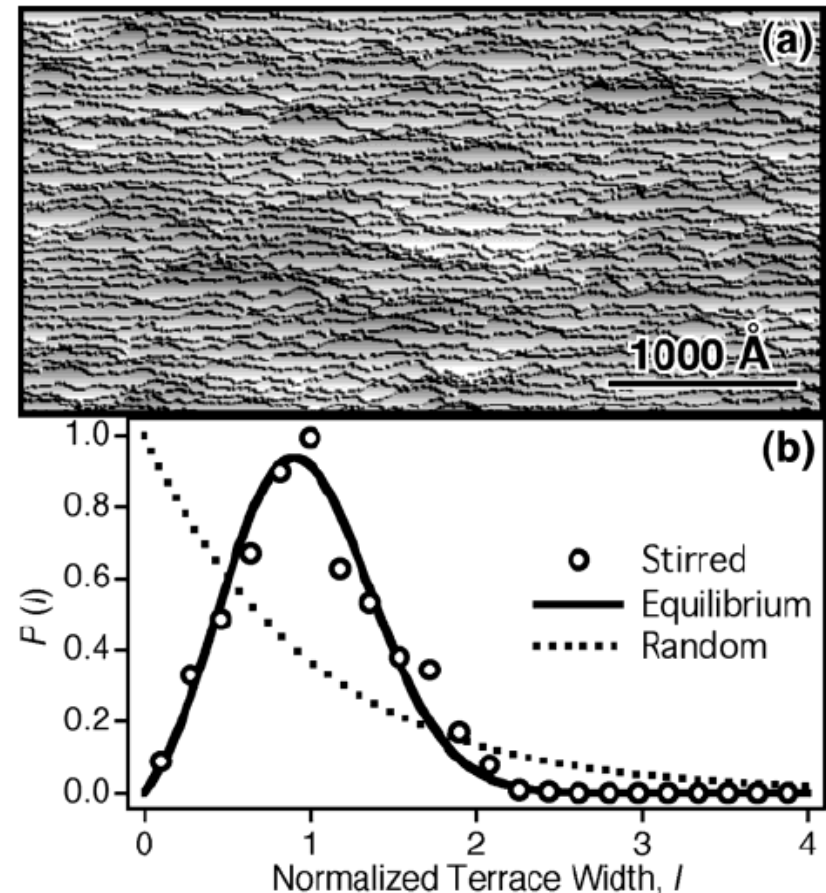
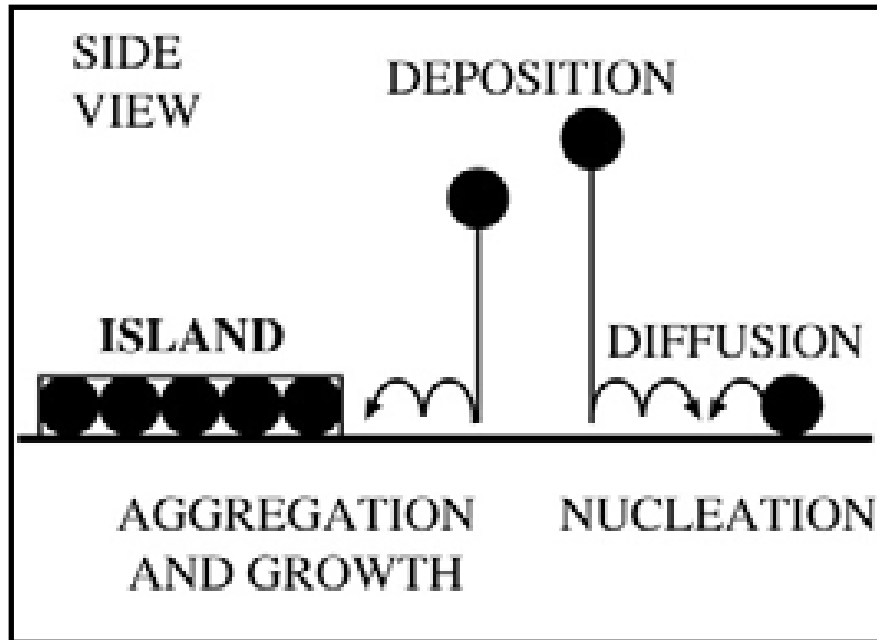


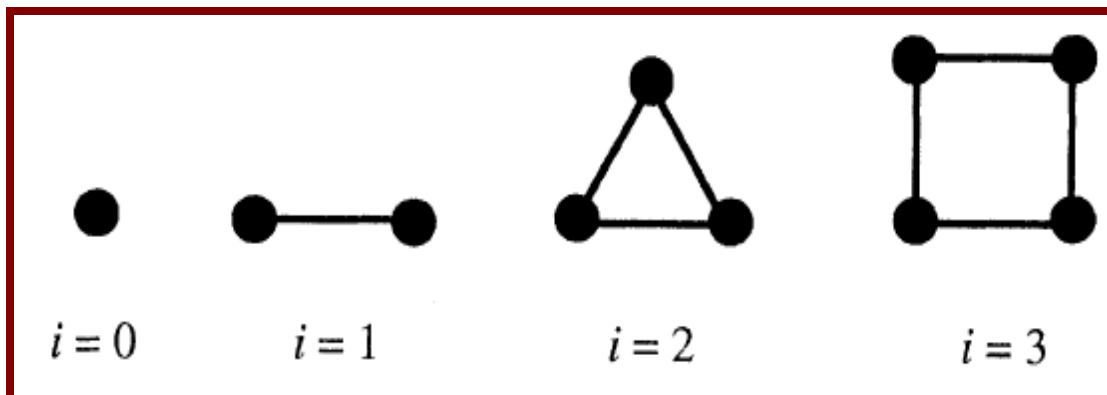
Figure 5. In the absence of diffusion-induced inhomogeneities, anisotropic step etching leads to relatively smooth surfaces, as shown by both the (a) steady state morphology and (b) terrace width distribution.

Description of deposition and island growth



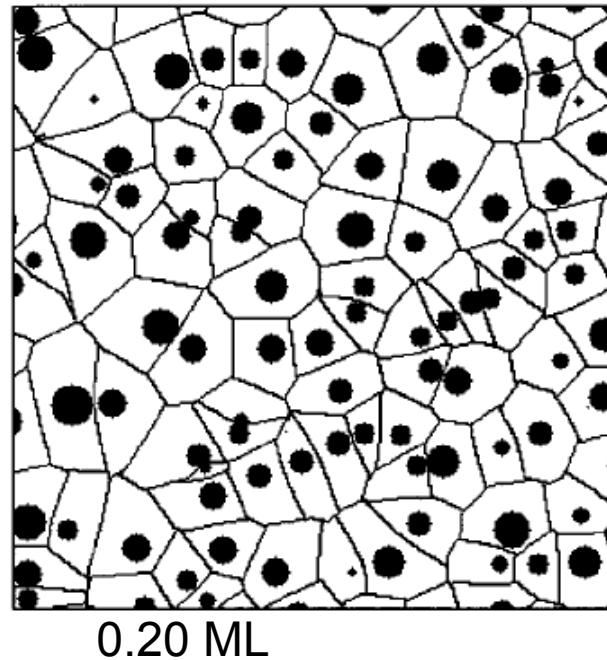
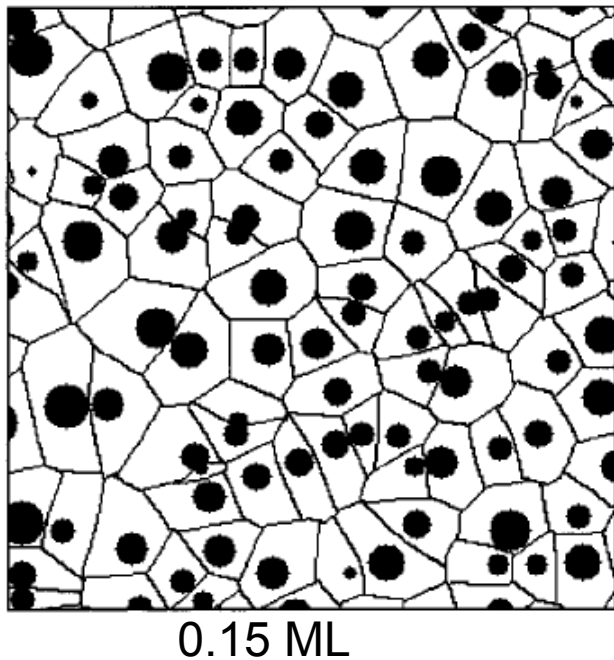
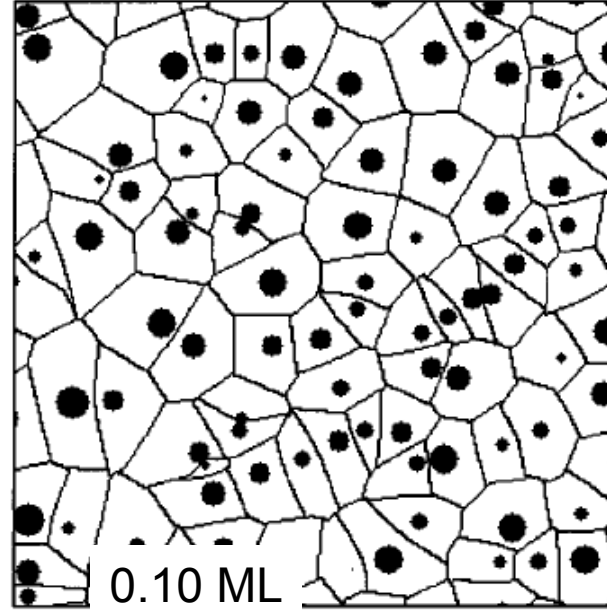
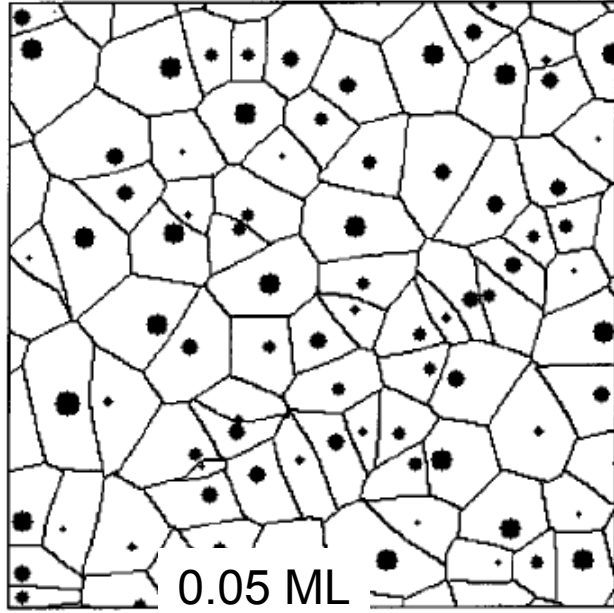
- Atoms deposited randomly
- Then diffuse till they meet
- Nucleate island, which grows
- But small islands can break up

J.W. Evans *et al.*, Surf. Sci. Rept. 61 ('06) 1



$i+1$ atoms: smallest stable island: *critical nucleus*

So i is size of largest unstable cluster

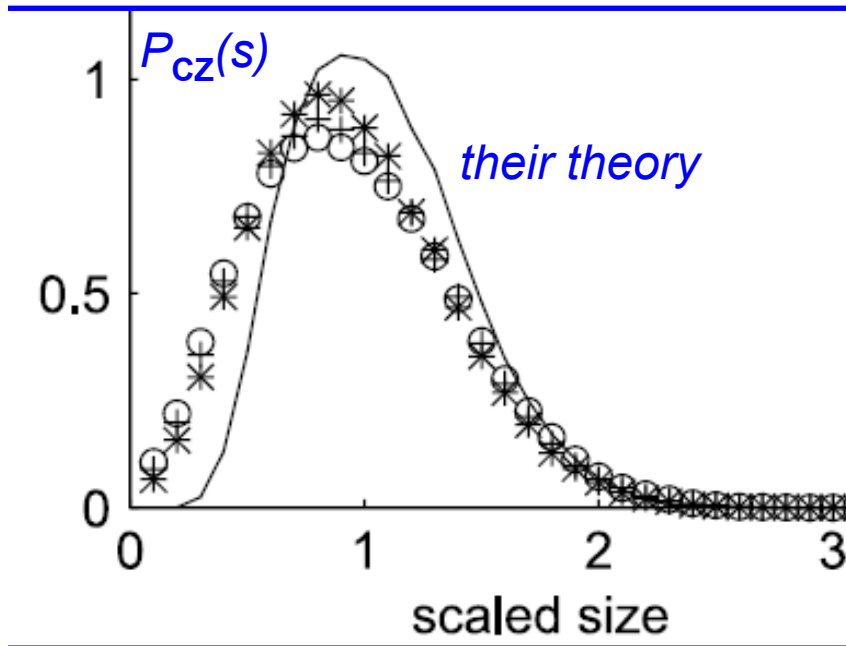


Evolution of Island Structures: Simulations of *Circular Islands*

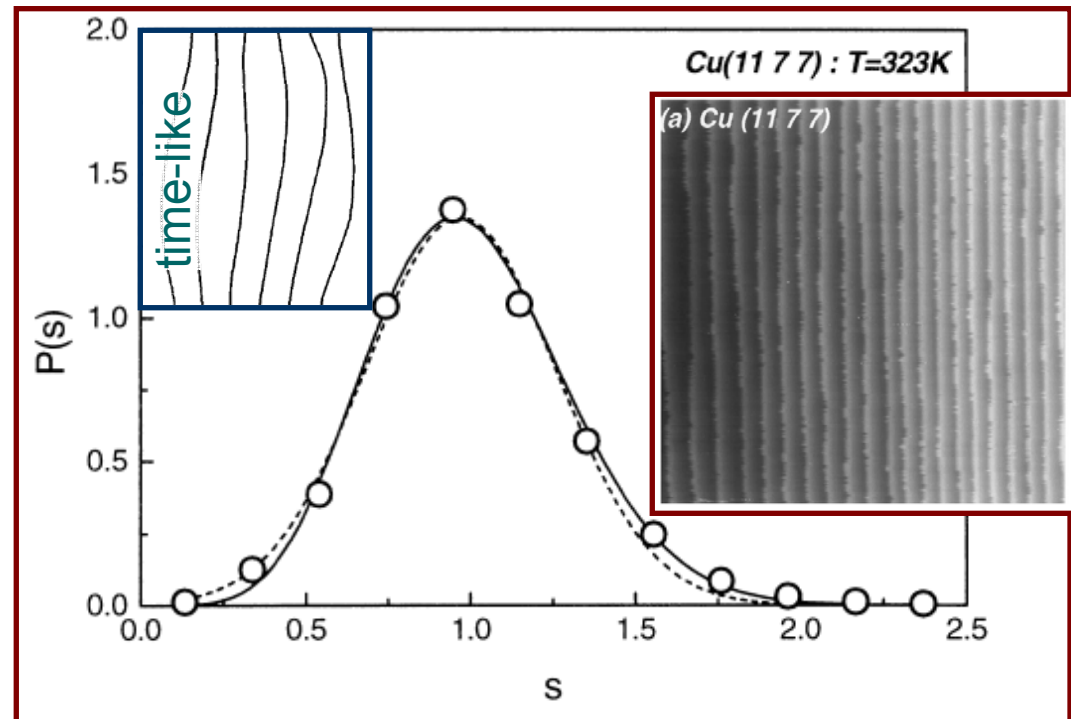
Mulheran & Blackman,
PRB 53 ('96) 10261

Can be more fruitful
to study distribution
of areas of *capture
zones (CZ)*
[Voronoi cells] than
of island sizes!

CZ distribution reminiscent of TWD (terrace-width distrib'n) on vicinals!



Mulheran & Robie, *EPL* 49 ('00) 617



Giesen & TLE, *Surf. Sci.* 449 ('00) 191

- Power-law rise (*from 0*), Gaussian decay
- Skewed, unlike Gaussian, but less so than popular gamma function
- Power-law exponent ρ (related to TWD *variance*) has specific physical meaning for TWD, for CZ also??

Scaling During Growth in 1D: Going Beyond Mean-Field Rate Eqns.

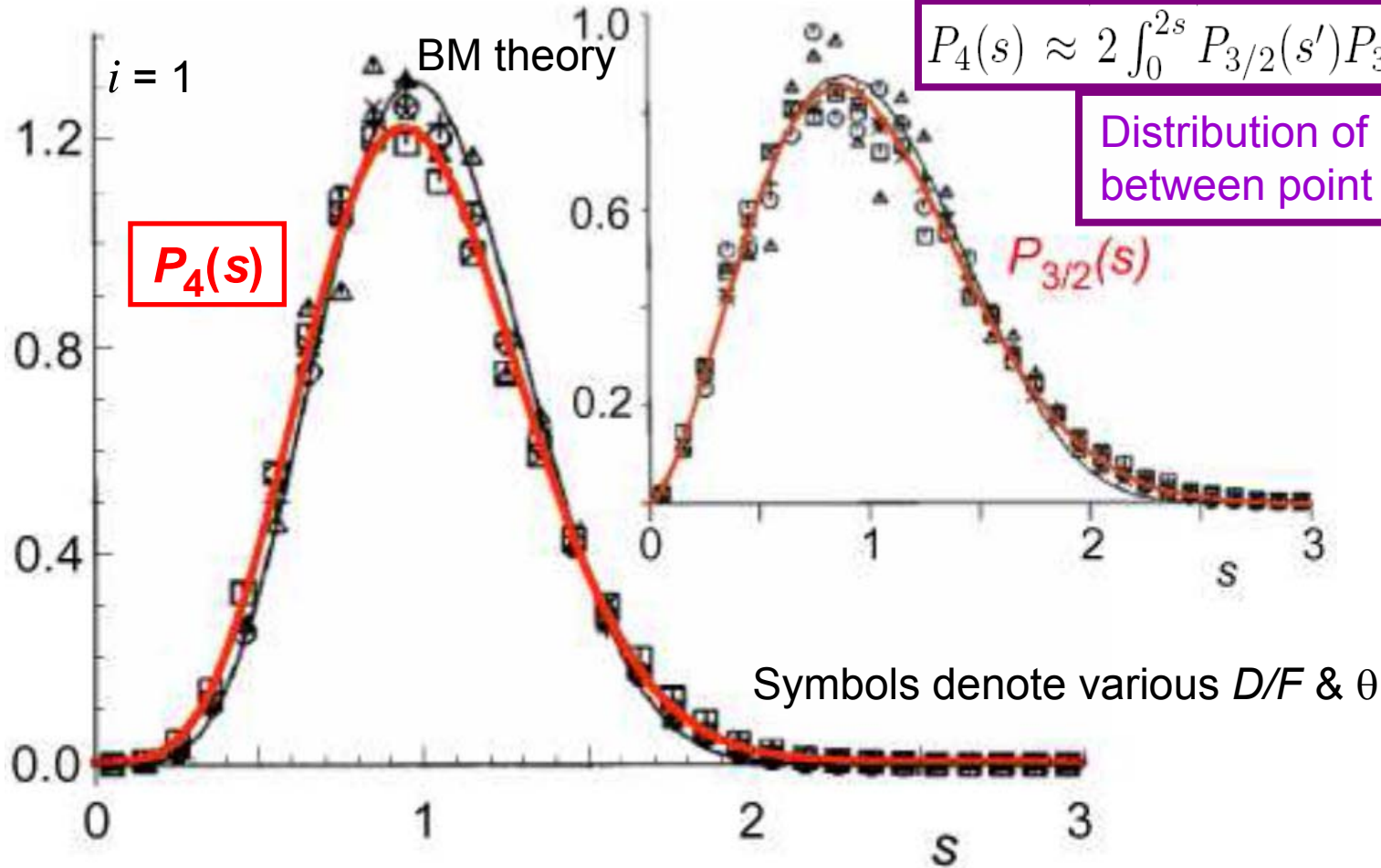
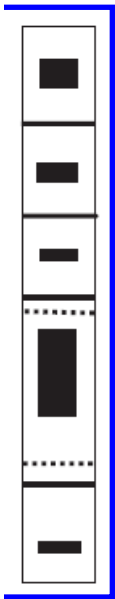
Blackman & Mulheran, PRB 54 (96) 11681

$P_4(s)$ fits numerical data at least as well as B&M's complicated theory expression (not expressible succinctly)

$$d = 1 \Rightarrow \rho = 2(i + 1)$$

$$P_4(s) \approx 2 \int_0^{2s} P_{3/2}(s') P_{3/2}(2s - s') ds'$$

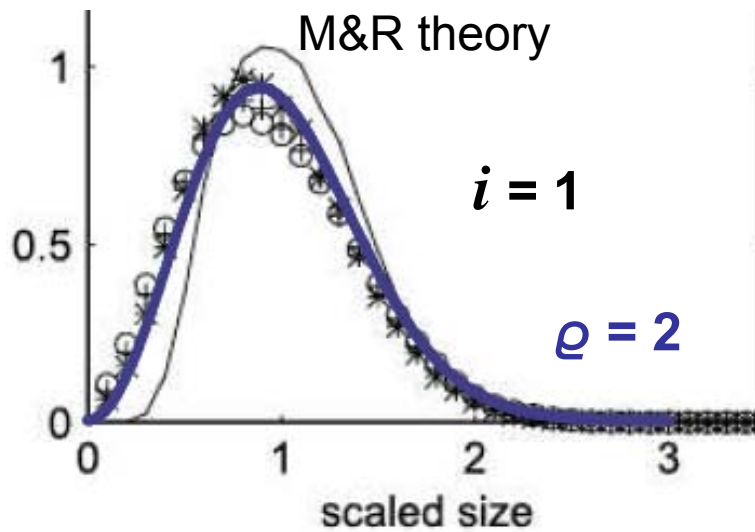
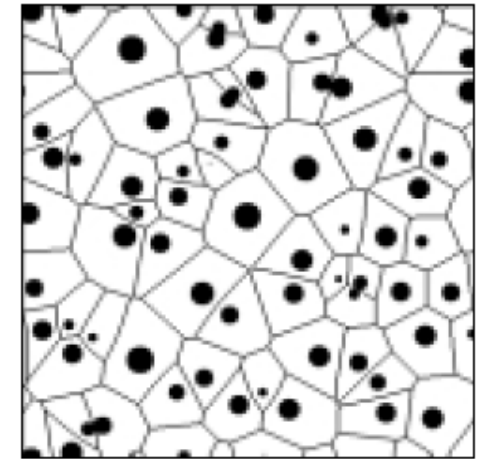
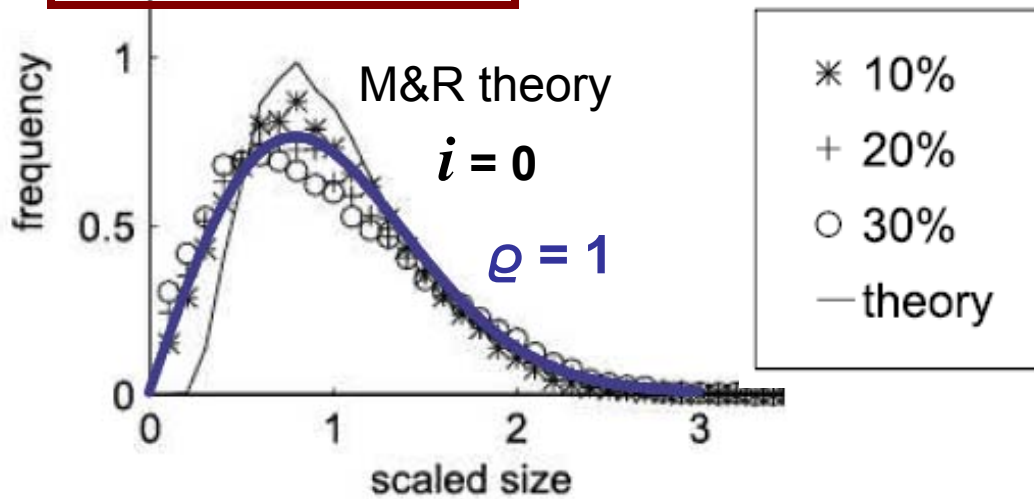
Distribution of gaps between point islands



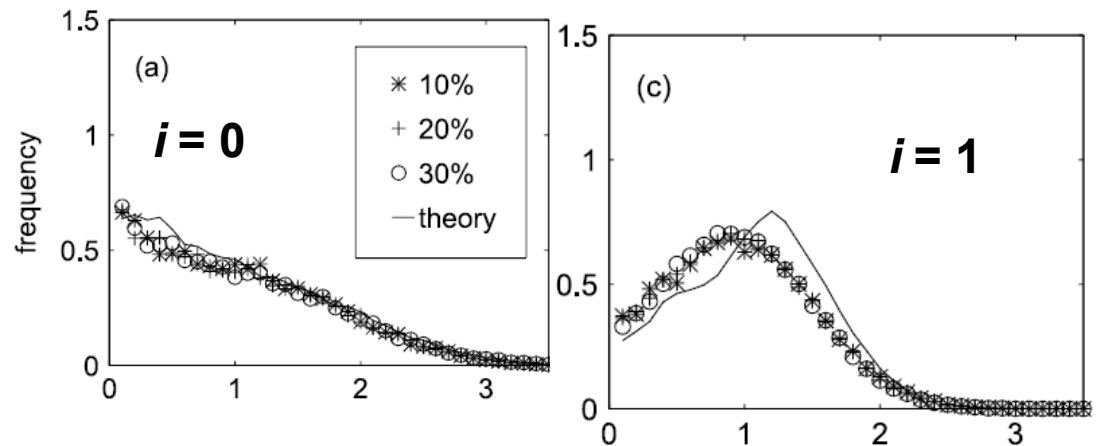
Theory of CZ size distributions in growth, *Mulheran & Robbie*, EPL 49(00)617

$d = 2 \Rightarrow \rho = i + 1$

Wigner distribution $P_\rho(s)$ fits much better than M&R theory



Island size distribution not so informative



Why it works: Phenomenological theory

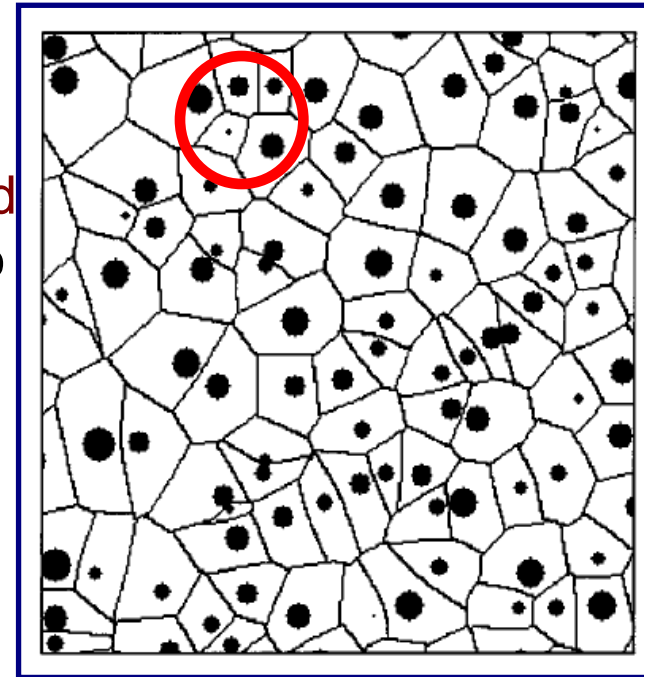
CZ does “random walk” with 2 competing effects on ds/dt :

1] **Neighboring CZs hinder growth** \Rightarrow external pressure
 leads to force opposing large s
 Also **noise** since atom can go to “wrong” island

2] Non-symmetric confining potential, **newly nucleated island has non-tiny CZ, comparable to neighbors** so force stops fluctuations of CZ to tiny values

3] Nucleation rate
 \propto adatom density \times density of critical nuclei
 \propto (adatom density)^($i+1$) [Walton relation]

4] **New CZ in region of very small CZs will have size comparable to those nearby, so very small also**



5] Combine to Langevin eq. $ds/dt = K \left[\frac{(2/d)(i+1)}{s} - Bs \right] + \eta$

Leads to Fokker-Planck eq.

with stationary sol'n $P_e(s)$

cf. AP, HG, & TLE, PRL 95 ('05) 246101

$$\frac{\partial P(s, \tilde{t})}{\partial \tilde{t}} = \frac{\partial}{\partial s} \left[\left(2bs - \frac{(2/d)(i+1)}{s} \right) P(s, \tilde{t}) \right] + \frac{\partial^2}{\partial s^2} [P(s, \tilde{t})]$$

Why it works: Phenomenological theory

CZ does “random walk” with 2 competing effects on ds/dt :

1] Neighboring CZs hinder growth \Rightarrow external pressure, repulsion B
leads to force $-KBs$ Also noise η

2] Non-symmetric confining potential, new island nucleated with
large size so force stops fluctuations of CZ to tiny values
In Dyson model, logarithmic interaction, so $+K(\)/s$

3] Can argue in 2D that $(\)$ is $i + 1$
using critical density $\propto s^i$, # sites visited in lifetime $\propto s^1$
entropy \propto - product s^{i+1} , & force $-\partial(\text{entropy}) / \partial s$
[Also $i + 1$ in 3D & 4D; but $2(i + 1)$ in 1D]

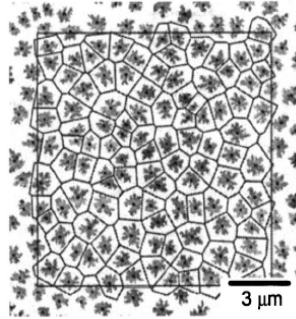
$$\begin{aligned} \dot{N} &= \sigma n N_i = \sigma n^{i+1} \\ \sigma &= D / \ell^{2-d} \quad s \equiv \ell^d \\ n &\propto \ell^2 \approx s^{2/d} \\ \text{prod} &\propto s^{(2/d)(i+1)} \end{aligned}$$

4] Combine \Rightarrow Langevin eq. $ds/dt = K [(2/d)(i + 1)/s - Bs] + \eta$ [$d=1,2$]

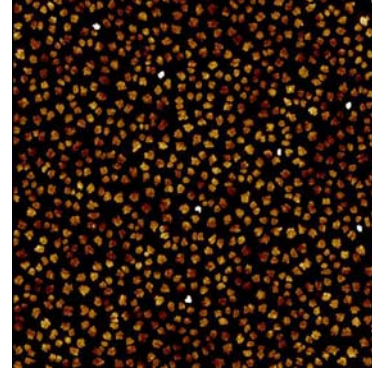
5] Leads to Fokker-Planck eq. with stationary sol'n $P_{\ominus}(s)$
cf. AP, HG, & TLE, Phys. Rev. Lett. **95** (05) 246101

Applications to actual (not MC) experiments

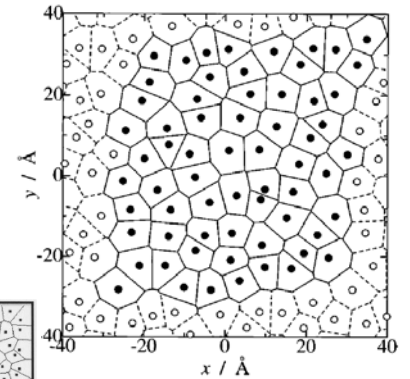
- Pentacene/SiO₂



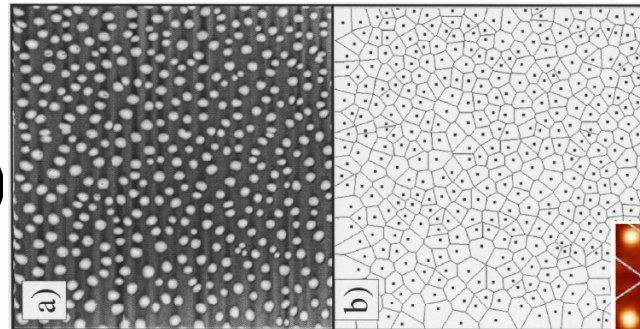
- Pentacene-PentaceneQuinone



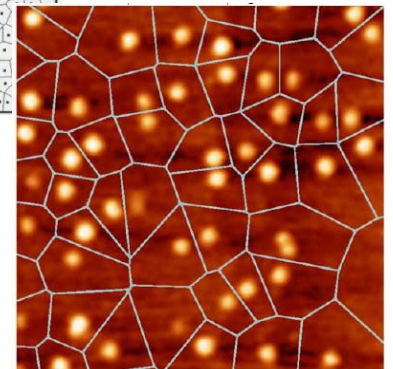
- Membrane area fluctuation in lipid bilayer



- Alq₃ on passivated Si(100)



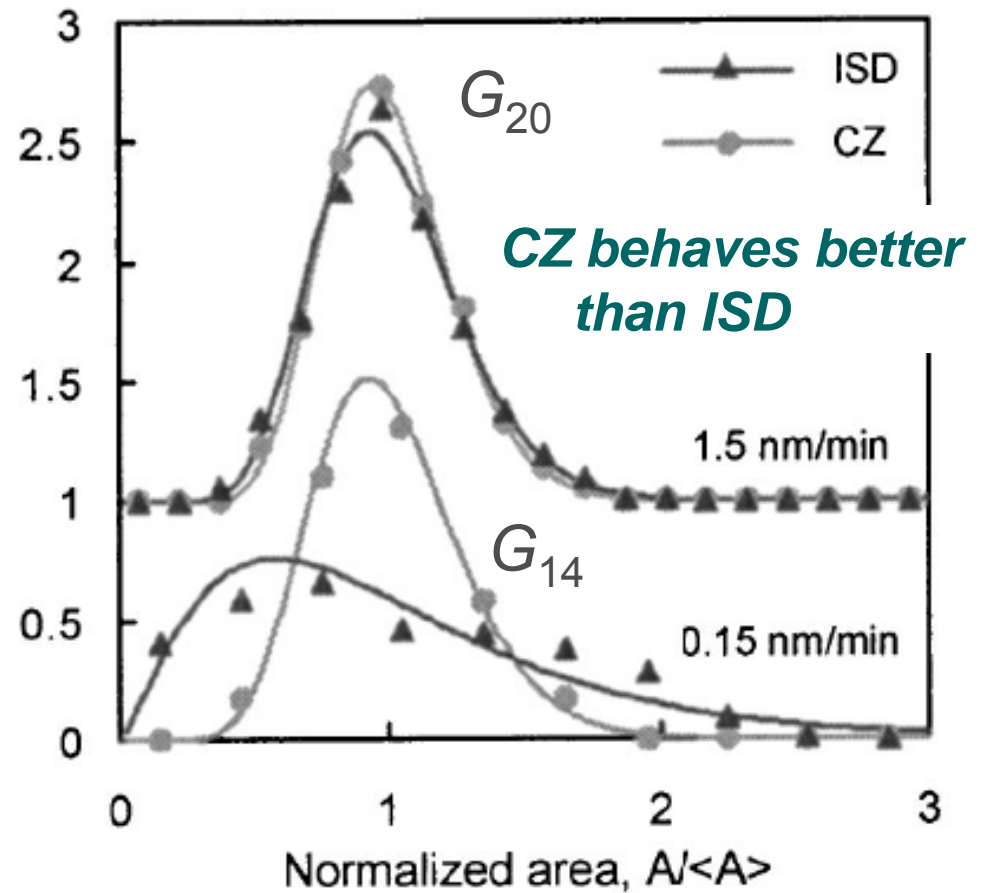
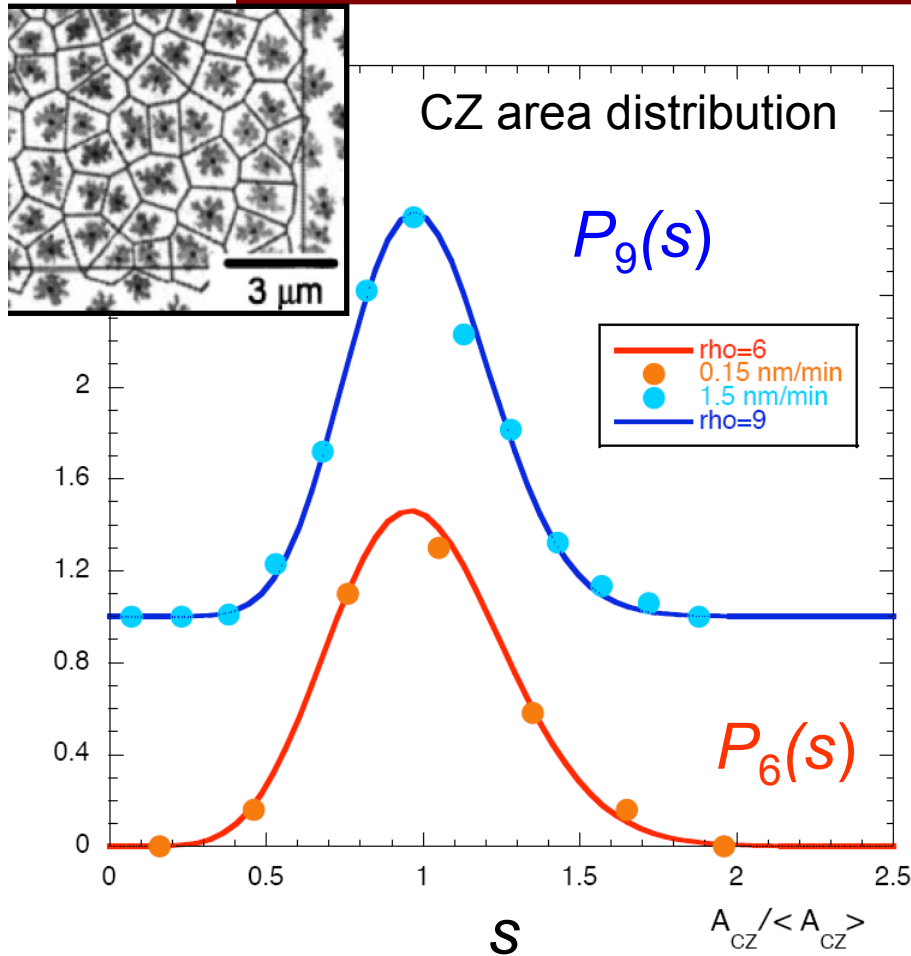
- InAs quantum dots on GaAs(001)



Exp't: Pentacene/SiO₂ Pratontop et al., 69 ('04) 165201

$$G_{\alpha}(x) = [\alpha^{\alpha}/\Gamma(\alpha)] x^{\alpha-1} \exp(-\alpha x)$$

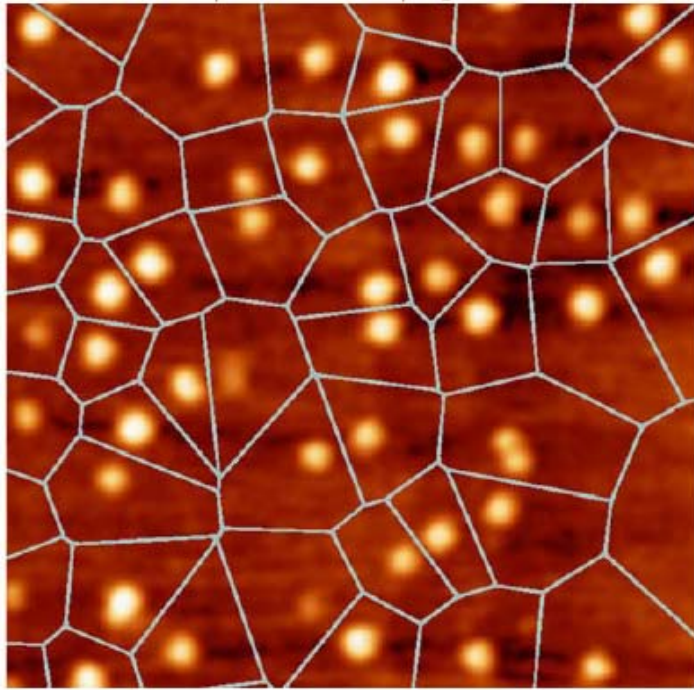
$G_{2\rho+\alpha_0}(s) \approx P_{\rho}(s)$ but G more skewed



For large ρ little difference in fit quality with GWS, Gamma or Gaussian.
But notable difference in philosophy and what one learns!

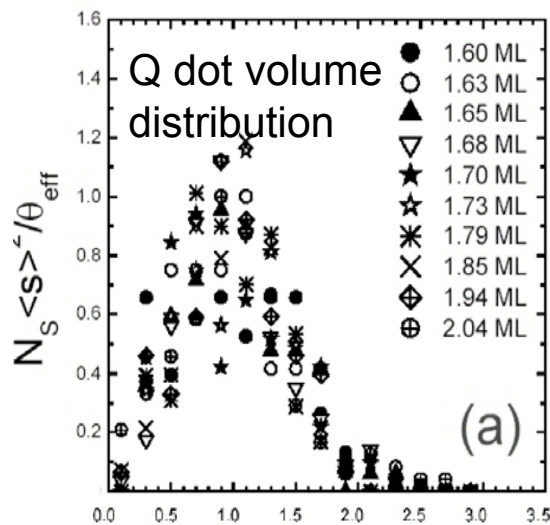
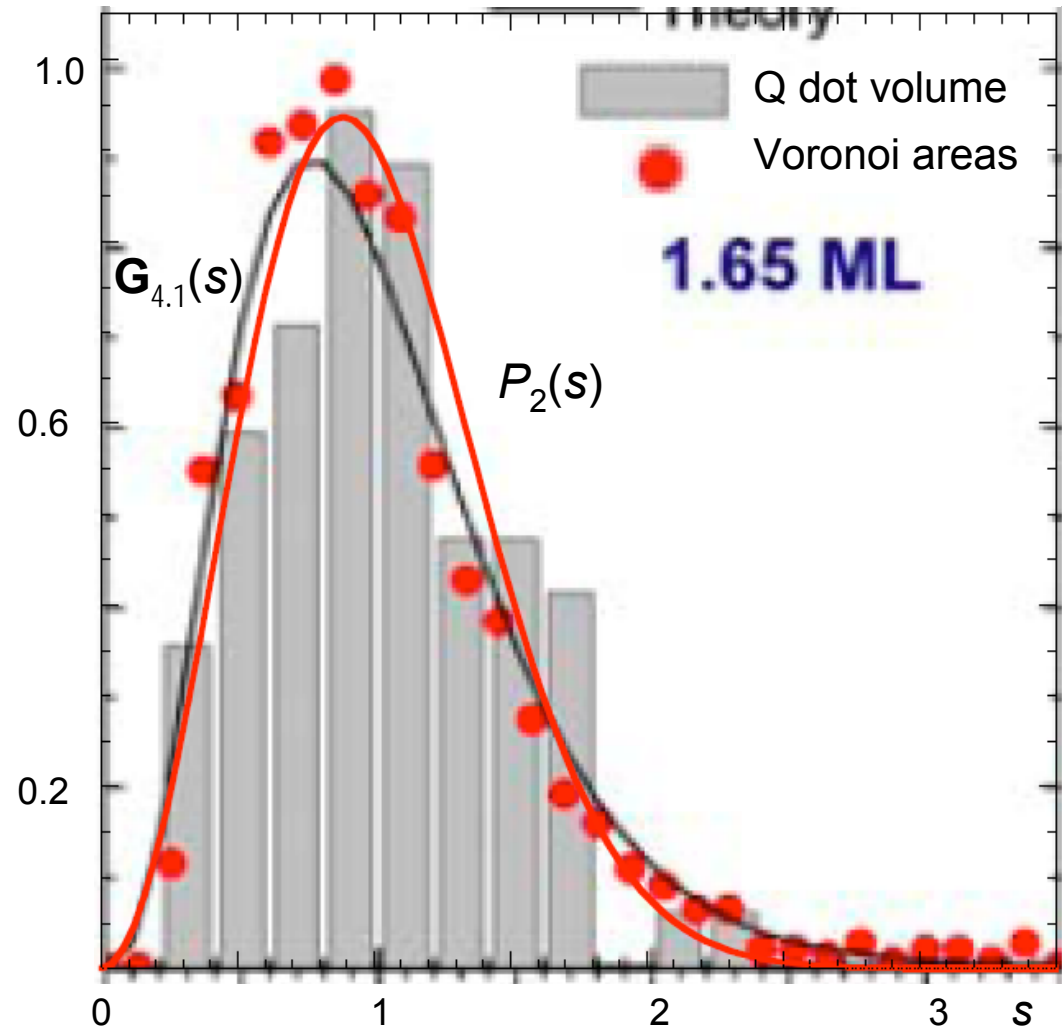
Scale invariance in thin film growth: InAs *quantum dots* on GaAs(001)

M. Fanfoni *et al.*, PRB **75** ('07) 245312



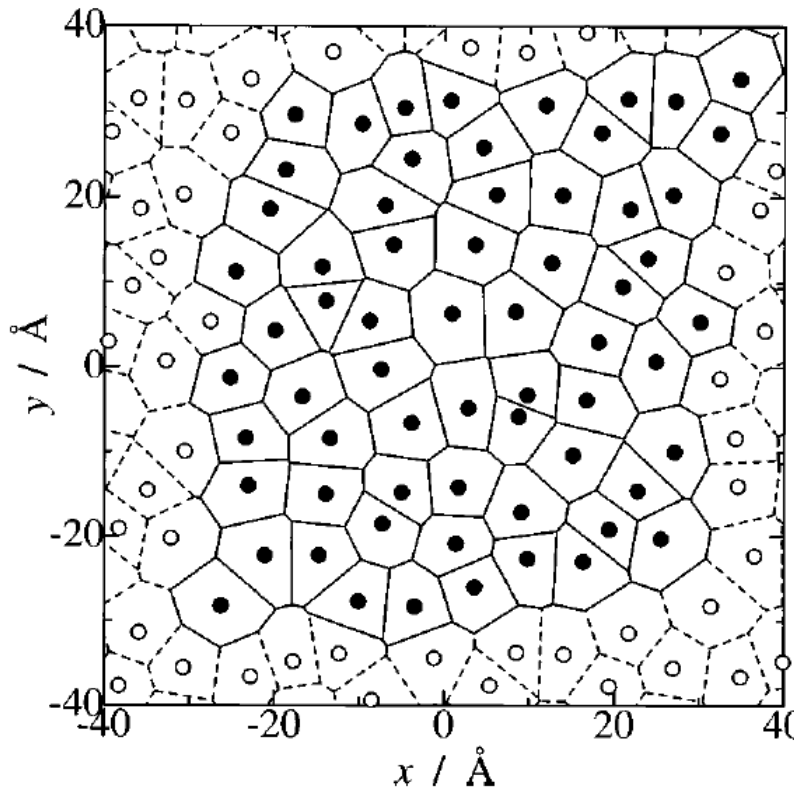
AFM, 1.68 ML, 350x350nm², 500°C

Θ (ML)	1.65	1.68	1.70	1.73	1.79	1.85
α	4.1	4.6	4.5	4.7	4.5	4.6

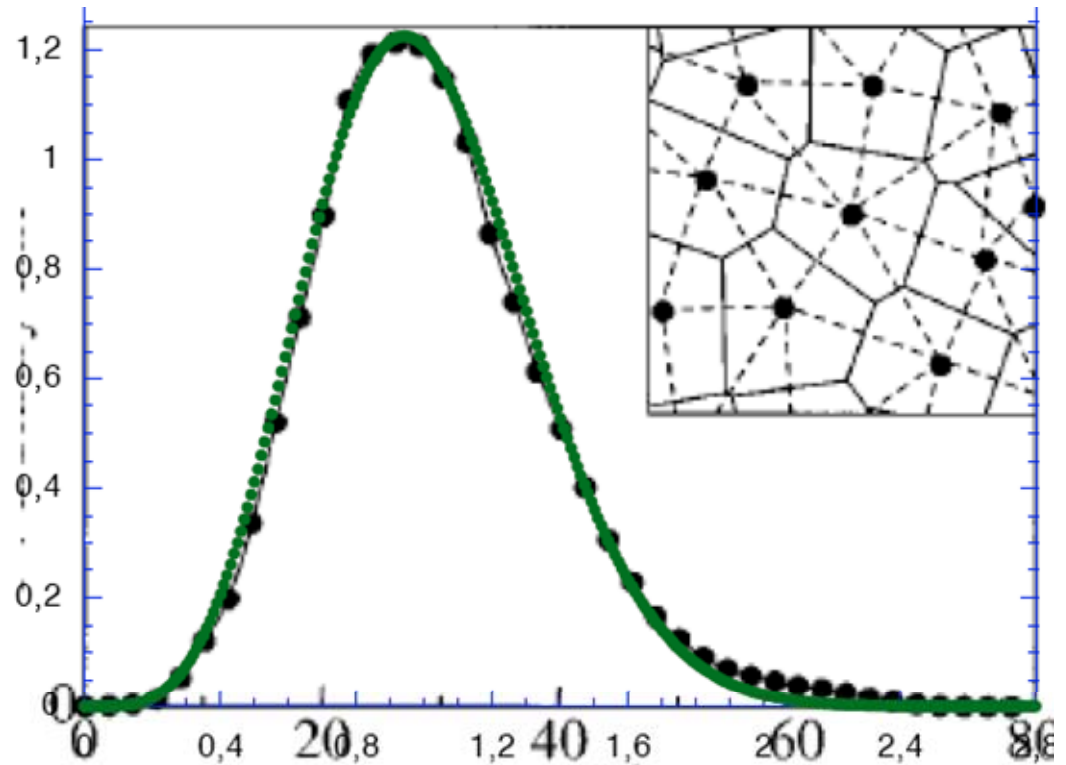


Membrane area fluctuation in lipid bilayer: Voronoi analysis

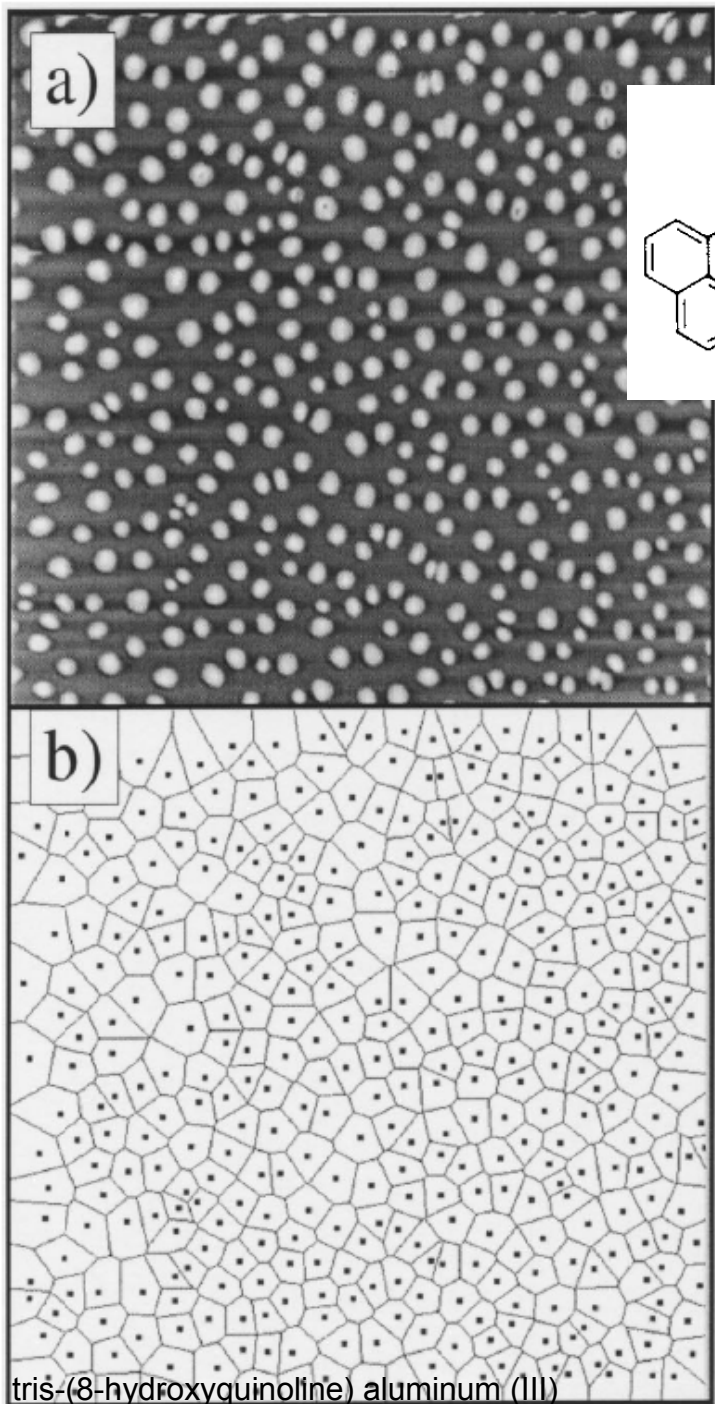
W. Shinoda & S. Okazaki, JCP 109 ('98) 1517



Voronoi tessellation for x-y projection of centers of mass of lipid molecules in upper half of bilayer



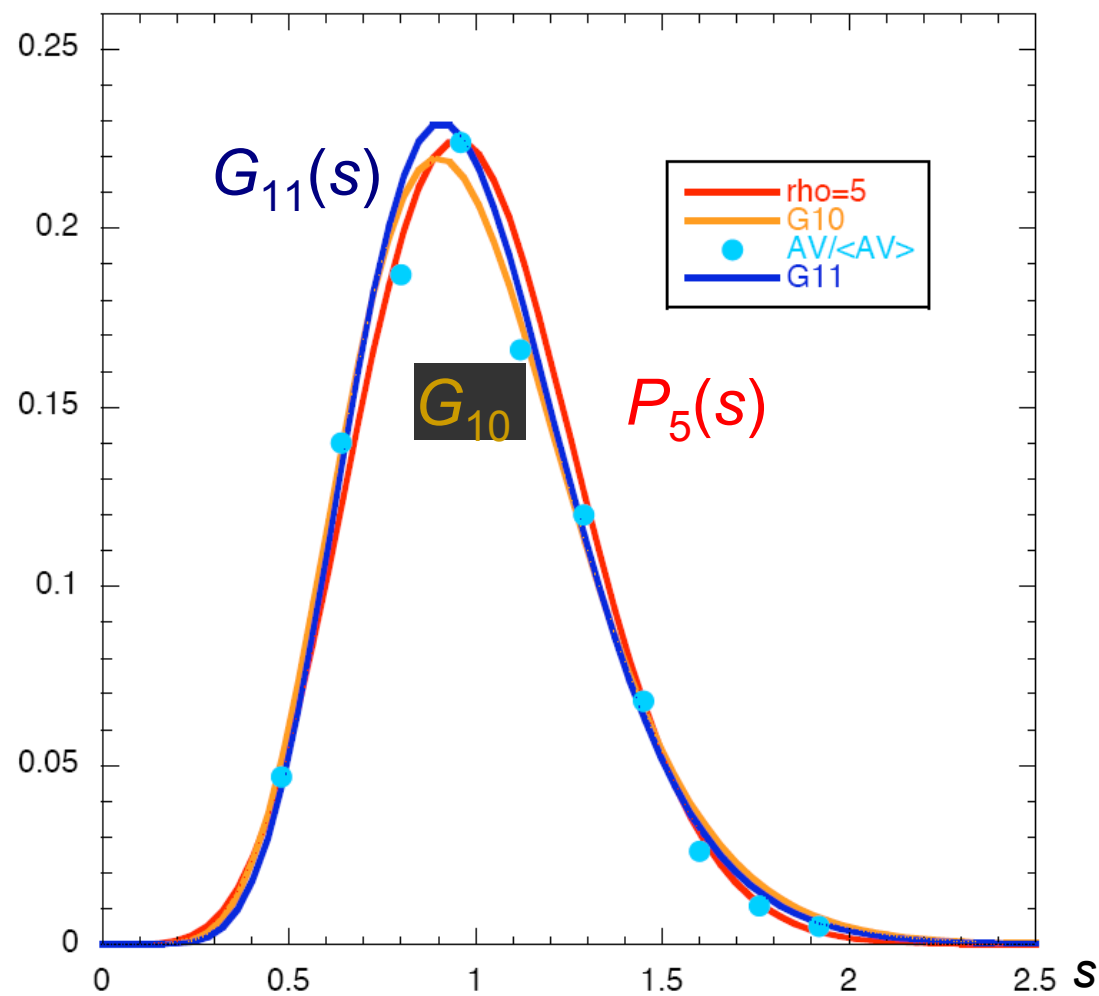
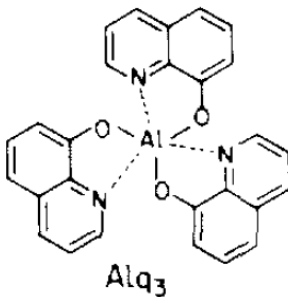
Distribution of area of triangle formed by 3 adjacent lipid molecules. Dashed lines in inset show triangles analyzed.



tris-(8-hydroxyquinoline) aluminum (III)

5 nm film Alq_3 on passivated Si(100), $T_s = 398\text{K}$

Brinkmann et al., PRB 66 ('02) 165430



Summary (see <http://www2.physics.umd.edu/~einstein>)

- TWD of vicinals provides physical entrée to intriguing **1D fermion models** & RMT, can connect to many other current physics issues --- universality in fluctuations --- Wigner surmise for 3 special cases based on explicit or implicit symmetry
- Generalized Wigner surmise $P_\varrho(s) = a s^\varrho e^{-bs^2}$ easy to use & describes universal fluctuations \Rightarrow broad applications
- For TWD width $\varrho = 1 + (1+4\tilde{A})^{1/2} \Rightarrow$ strength of elastic repulsion
- Fokker-Planck derivation & application to relaxation of steps from arbitrary initial configurations
- Focus on **distribution of areas of capture zones**, rather than island sizes; $\varrho = i + 1$ [or $2(i+1)$ in 1D] \Rightarrow critical nucleus

TLE, Appl. Phys. A **87** ('07) 375

AP, HG, & TLE, PRL **95** ('05) 246101

AP & TLE, PRL **99** ('07) 226102

ABH, AP, & TLE, JPCM ('08) & preprint